Effects of an Osseointegrated Above-The-Knee Prosthesis on Gait and Balance in Transfemoral Amputees

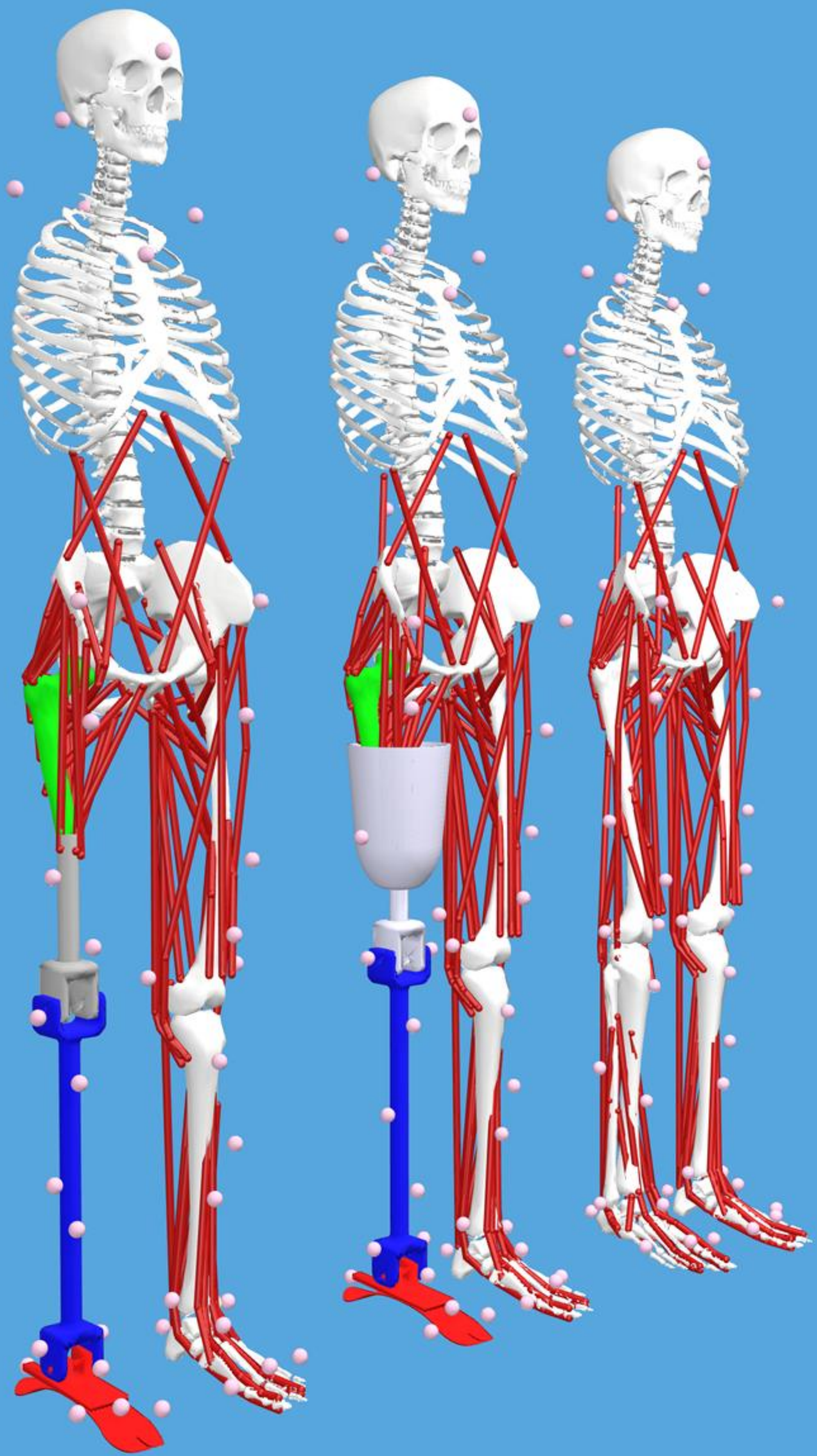

MSc Thesis Technical Medicine

Alexander Hendrik Kuipers

Universiteit Leiden The Netherlands
TU Delft Delft University of Technology
Erasmus University Rotterdam

This page was intentionally left blank

EFFECTS OF AN OSSEOINTEGRATED ABOVE-THE-KNEE PROSTHESIS ON GAIT AND BALANCE IN TRANSFEMORAL AMPUTEES

Alexander Kuipers

Student number : 4864808

October 10th, 2025

Thesis in partial fulfilment of the requirements for the joint degree of Master of Science in

Technical Medicine

Leiden University ; Delft University of Technology ; Erasmus University Rotterdam

Master thesis project (TM30004 ; 35 ECTS)

Department of Trauma Surgery

Rotterdam Erasmus Medical Centre
January 2025 – October 2025

Supervisor(s):

Prof. dr. ir. J. (Jaap) Harlaar	Technical Supervision
Dr. M.G.H. (Mariska) Wesseling	Technical Supervision
Dr. Lt. Col. O.J.F. (Oscar) van Waes	Medical Supervision

Thesis committee members:

Prof. dr. ir. J. (Jaap) Harlaar, Erasmus MC, Department of Orthopaedics (Chair)

Dr. Lt. Col. O.J.F. (Oscar) van Waes, Erasmus MC, Department of Trauma Surgery

Prof. dr. H.E.J. (DirkJan) Veeger, TU Delft, Department of BioMechancial Engineering

Abstract

Introduction Lower-limb amputations often result from vascular or traumatic causes and substantially affects mobility and quality of life. Traditionally, rehabilitation has relied on socket prostheses (SP), but are limited due to discomfort, skin irritation, and inefficient load transfer at the socket-skin interface. Osseointegrated prostheses (OIP) is an alternative, which directly anchors a titanium implant in the residual bone, to which the prosthesis can be attached. This direct connection improves mechanical feedback, comfort, and functional mobility. Research indicates that OIP users demonstrate enhanced proprioception, increased walking efficiency, and greater gait symmetry compared to SP users, although outcomes vary across individuals. Despite this, long-term biomechanical adaptations and objective measures of gait and balance performance have yet to be clearly established. To address this gap, the present study aims to identify biomechanical biomarkers of gait and static balance in transfemoral amputees with an OIP compared to SP and able-bodied controls, using quantitative gait and balance analysis.

Methods This cross-sectional observational study was approved by the Erasmus MC Ethics Committee and conducted in accordance with the Declaration of Helsinki. 13 Participants visited the Erasmus MC for a testing session. Gait and balance were measured with a motion capture system and a dual-belt treadmill with integrated force plates. The CGM 2.5 was used for the marker protocol, with slight adjustments. Tests included walking at self-selected and imposed (1 m/s) speeds, and static balance tasks under three varying sensory and cognitive conditions. OpenSim models of the control and OIP groups were adapted for this study, while the SP model was generated by modifying the OIP model with a socket interface. Marker data and ground reaction forces were recorded and processed in OpenSim 4.5 using personalized models to compute kinematics, kinetics, and spatiotemporal parameters. Additional balance parameters, such as Margin of Stability in gait and Centre of Pressure, were calculated to evaluate balance control and load distribution between the non-affected and affected side.

Results At both imposed and self-selected speeds, OIP users demonstrated gait patterns closer to healthy controls than SP users. Both prosthetic groups exhibited reduced knee flexion during loading and showed asymmetrical stance times, with longer stance on the intact limb. OIP users showed improved load transfer and stability, whereas SP users displayed greater asymmetry, lower cadence, and longer step lengths. Kinematic and kinetic analyses revealed lower ankle push-off and knee flexion moments in both groups, compensated by increased hip and trunk involvement. Margin of Stability values in gait suggested more favourable mediolateral stability in OIP users, while balance trials indicated greater reliance on visual input and non-affected limb loading in SP users.

Conclusion The findings in this study show that osseointegration enhances gait symmetry and stability compared to socket prosthesis, though not fully restoring natural movement. Current compensation strategies highlight the need for focused rehabilitation and further investigation into the long-term functional and musculoskeletal effects of both prosthesis types.

Keywords: Osseointegration, Socket prostheses, Musculoskeletal modelling, Above-the-knee amputation, Gait, Balance

Table of Contents

List of Abbreviations

AP	Anteroposterior
BoS	Base of Support
CoM	Centre of Mass
CoP	Centre of Pressure
DoF	Degree of Freedom
fBoS	functional Base of Support
GRF	Ground Reaction Force
HC	Healthy Controls
ID	Inverse Dynamics
IK	Inverse Kinematics
IS	Imposed Speed
LLA	Lower-limb amputation
ML	Mediolateral
MOBI	MOtion Biomechanics & Imaging
MoS	Margin of Stability
MPK	Microprocessor-Controlled Prosthetic Knees
NA	Non-affected
OI	Osseointegration
OIP	Osseointegrated Prosthesis
RMS	Root Mean Square
SD	Standard Deviation
SI	Symmetry Index
SP	Socket Prosthesis
SSS	Self-Selected Speed
TFA	Transfemoral Amputee
TTA	Transtibial Amputee
TUG test	Timed Up and Go Test
vGRF	Vertical Ground Reaction Force
XCoM	Extrapolated Centre of Mass

1. Introduction

Yearly, in the Netherlands alone, around 3300 lower-limb amputations (LLA) are performed (1). Around 90% of transfemoral (TFA) and transtibial (TTA) amputations are caused by vascular problems such as diabetes, while roughly 5% are due to cancer (1). The remaining cases find its origin in traumatic causes, such as traffic accidents.

Due to the growing and aging population, which increasingly becomes more obese, the amount of people suffering from diseases related to blood vessels, such as diabetes increases (2). Therefore, more people may require a lower-limb amputation in their lifetime, primarily due to diabetic neuropathy or impaired circulation caused by peripheral arterial disease (PAD). Amputations for the lower limb can be classified per location of the amputation, from toes up to the hip. Although at all levels appropriate prosthesis treatment will greatly restore mobility, a more proximal amputation yields lower motor performance in keeping balance or walking speed, as measured with the six-minute walk test (6MWT) and the timed up and go (TUG) test (3-5). To retain mobility, individuals with LLAs often use prostheses. Prosthetic limbs have been used for centuries, interfaced to the body by a socket that tightly fits the stump, known as a socket prosthesis (SP) (6).

The first prosthesis found, a wooden and leather toe in the 15th century BC, comes from a time when prostheses were not only developed for function, but also for cosmetic and spiritual purposes. By 300 BC, more practical prosthetics, such as wooden legs, were created to enable Roman soldiers to return to battle. Throughout the centuries, prosthetics continued to evolve, and in the 16th century Ambroise Paré designed hand and legs prostheses that used mechanical mechanisms, allowing amputees to regain greater functional mobility. These early prosthetics laid the foundation for more advanced artificial limbs used today. Improvements include lightweight metals and plastics, which offer more comfort and functionality to the user (7). In the late 20th century, developed began creating microprocessor-controlled prosthetic knees (MPKs), with companies as Blatchford and Ottobock releasing the first commercially available models (Blatchford Intelligent Prosthesis (IP) Knee and Ottobock C (computerized)-leg) (8, 9). MPKs use sensors and microprocessors to continuously monitor gait and adjust knee resistance in real time, marking a significant shift in technology. The development of MPKs continue to this day, with improvements in sensor accuracy, gait cycle detection, terrain accommodation, force accommodation, and speed accommodation. These innovations allow for user-specific movements, increased stability on uneven terrain, and greater functionality during daily activities. Advanced features such as powered knee flexion and extension have further improved stability and comfort, making MPKs a crucial part of modern prosthetics for lower leg amputees (10).

Although the developments of prosthetic limbs have given amputees an increased mobility, still some problems remain, primarily at the socket-skin interface, which remains a point of concern in prosthetic design and use. Problems include:

1. **Force-transfer**
   In humans, forces are normally transmitted through the skeleton and bones. But in amputees using a SP, forces must be transferred between the prosthesis and the residual limb via the socket. These forces are transferred to the residual femur through the skin, which is not meant to bear weight (11). This mismatch between load-bearing requirements of the prosthesis and the limited capacity of the skin to comfortably withstand loading, leads to discomfort and complications, especially if there is pressure in pressure-sensitive areas (11).
2. **Skin issues**
   To ensure stable attachment, a snug fit between the socket and residual limb is essential. But, as there is weight-bearing on the affected leg, pressure applied to the skin leads to friction and heat, which in turn can also lead to sweating, leading to skin issues. These include conditions such as blisters, redness and ulcers. Problems are worsened by daily changes in size and shape of the stump, which are due to the temperature changes, hydration and physical activity. And as a result, increases pain and

discomfort, limiting the ability of amputees to wear the prosthesis for longer periods of time and decreasing overall quality of life (12-16).

3. **Sitting discomfort**

   This pressure can cause significant discomfort or pain, limiting the amputee's ability to sit for extended periods. As a result, some amputees may be forced to remove the prosthesis in order to sit comfortably, reducing overall prosthesis use and impacting daily activities (17).

To address these issues, an alternative approach has been developed: a relatively new method known as osseointegration (OI), which involves directly anchoring the prosthesis to the residual limb through integration with the bone. The principle of OI was noted between 1940 and 1952, but pioneered in dentistry, where Dr. Per-Ingvar Brånemark, discovered the biocompatibility of titanium with bone, applying the concept for dental implants (18, 19). It was defined by Dr. Brånemark as "the formation of a direct structural and functional connection between ordered, living bone and the surface of a load-carrying implant" (20). The first successful OI dental implantation was performed in 1965 where patients with total loss of all teeth regained oral function after OI (21). Osseointegrated prostheses (OIP) in rehabilitation of amputees started in the 1990. This was based on research performed by Rickard Brånemark, son of Dr. P.I. Brånemark (22). At first, it was tested in animals, whereafter the first OIP could be performed in a 25-year-old woman with a bilateral TFA (22, 23). Traditionally, OI is performed in two stages, where in the first stage the fixture component is implanted intramedullary, and is given time to completely integrate with the bone. During a second surgery, a percutaneous opening is made, so the abutment can be connected to the fixture. An alternative is the one-stage approach, in which implantation of the fixture and connection of the abutment is performed in one procedure (24). The two-stage approach is well-documented and offers long-term data. In contrast, the one-stage approach allows for quicker recovery and fewer infections, but it comes with trade-offs in terms of long-term outcomes and fracture risks (24).

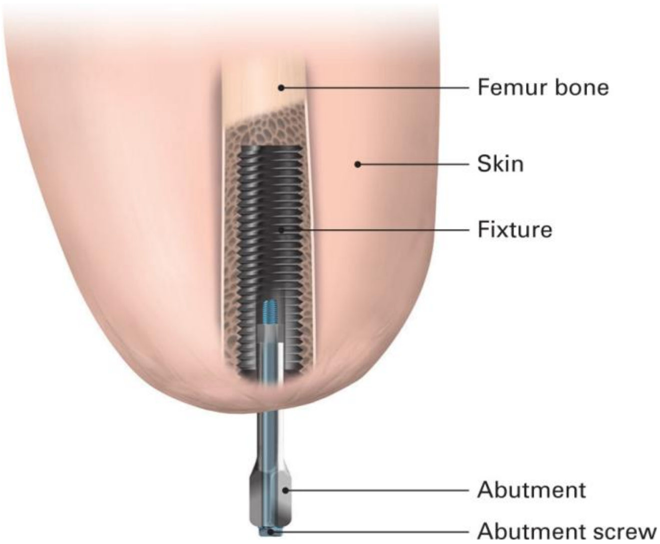

Figure 1: Schematic view of the fixture inserted in the femur, and the abutment, which are hold together by the abutment screw. Copied from Hagberg et al. (2020) (26)

Different types of fixtures exist, such as the screw-fit OI, of which an illustration shown in Figure 1, which shows the fixture (a threaded titanium implant), the abutment (the skin-penetrating cylindrical implant) and the abutment screw, which holds the system together (25). An alternative design, the press-fit fixture, is shown in Figure 2 (26).

Once the fixture and abutment have been successfully implanted, through the one-stage or two-stage approach, the remaining components can be attached to the abutment. These components include the taper base, bushing, bushing screw and adapter. One of the most used OI-systems is the Osseointegrated Prosthetic Limb (OPL) by Permedica s.p.a (Milan, Italy), shown in Figure 2. Through the final adapter, the external knee prosthesis is attached, allowing the patient to start rehabilitation, weight-bearing, and restore functional mobility.

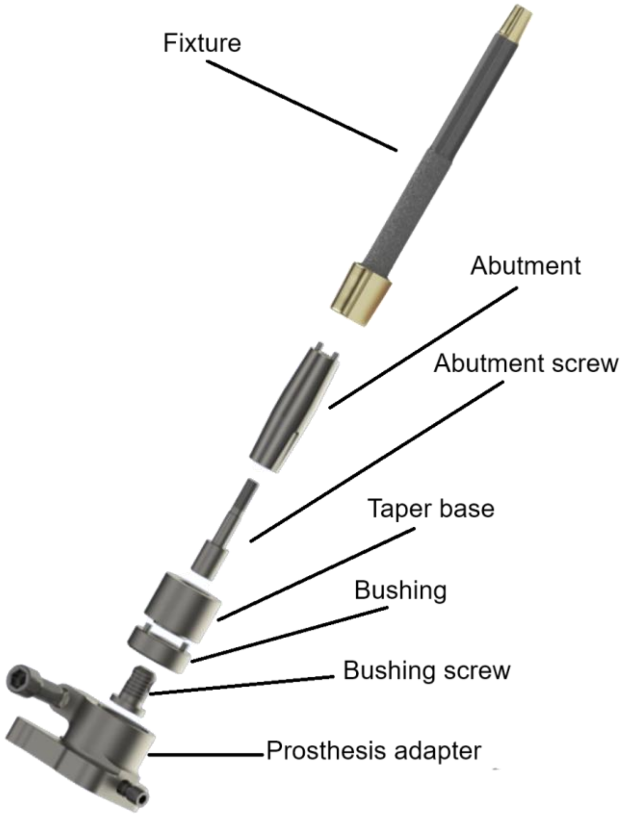

Figure 2: Components of the OPL (Permedica s.p.a; Milan, Italy) required to connect the prosthesis to the implant in the residual limb. The image shows the implanted components alongside the taper base, bushing, bushing screw, and prosthesis adapter. Adapted from The Osseointegration Group [Internet] (26).

One key advantage of an OIP is improved mechanical feedback, or osseoperception, provided by the direct connection between the prosthesis and the residual bone, which enhances proprioception. Studies showed that OI-users showed improvement in feeling forces, minimizing soft tissue interference, and adjusting during gait, supporting the claim of increased proprioception (27, 28). Toderita et al. (2024) reported improvements in gait symmetry and reduced compensatory movements (29). A case study by Leijendekkers et al. (2017) also highlighted improved gait and functional mobility in OIP users, further supporting the advantages of osseointegration (30). However, the prosthesis does pierce the skin, requiring regular cleaning to prevent infection at the stoma site (31). Additionally, a study among SP and OIP users reported that OIP users experienced greater comfort and longer prosthesis-wearing time, with usage time increasing 45% from 56 hours per week in SP users to 101 hours per week in OIP users (32). Besides these parameters, after full recovery following surgery, there have been significant improvements in functional parameters such as the 6MWT and the TUG test (32-34).

While OIP provides these benefits, certain factors influence patient eligibility. Diabetes Mellitus (DM) is a contraindication for OIP in TFAs, due to the vascular complications, limiting the ability to control infection at the stoma site (35). However, recent evidence (Hoellwarth et al., 2024) states that if DM is well-managed, TFA patients can also experience the benefits of an OIP (36). This could significantly increase the population for which OIP can be an alternative to SP.

Given these functional advantages and possibly expanded eligibility, it is important to examine how OIP influences gait, and how this relates to gait in SP patients. Altered biomechanics in amputees can lead to overloading of the intact limb and reduced residual limb loading. These changes may result in secondary musculoskeletal complications, highlighting the importance of assessing gait and postural control (37).

1.1 Walking

To better understand the biomechanical effects of walking with prosthetics, multiple studies have conducted biomechanical gait analyses, examining kinematic, kinetic, and spatiotemporal parameters. These studies compared different prosthesis groups, as well as pre- and post-surgical outcomes within groups (29, 38-41).
They collectively demonstrate that transitioning from SP to OIP can lead to measurable biomechanical changes. A longitudinal study by Ekdahl et al. (2025), following 19 amputees before and after OI, reported outcomes that after OI, there was an increased hip abductor force production and reduced hip flexor demand on the amputated side (39). This increase in force, led to a more symmetric muscle force between the intact and affected limb, particularly in the Gluteus Medius and Tensor Fasciae Latae, which contribute to hip abduction and internal rotation during the stance phase of the gait cycle.

Walking speed is one of the main indicators for walking ability. A study comparing SP and OIP found that OIP users had a walking speed of 1.03 ± 0.17 m/s, faster than SP users at 0.87 ± 0.17 m/s, but the differences were not statistically significant (42). However, van de Meent et al. (2013) reported significant improvements in OIP users compared to SP, including the ability to walk further and faster while using 18% less energy, indicating more efficient gait (32). Additionally, this study reported a decrease in hip flexion forces, leading to a greater asymmetry compared to SP, suggesting that OIP achieves propulsion using different hip strategies in each limb (39). However, other studies report shifts in load distribution toward the intact limb, resulting in greater cumulative limb and joint loading, along with persistent gait asymmetries (38, 40).

While some OIP users show improved mobility, gait patterns, loading patterns, and patient-reported outcomes, adaptations are variable, underscoring the need for targeted rehabilitation and long-term monitoring of joint health in OIP users (29, 38, 41).

1.2 Gait cycle

To analyse gait from longer recordings, multiple full gait cycles can be extracted. A gait cycle is defined as the period from initial contact (heel strike) of one foot until the next heel strike of the same foot. Within this cycle, the stance phase typically occupies about 60% of the cycle, while the swing phase accounts for the remaining 40%. Figure 3 illustrates a full gait cycle along with other important events within the cycle (43).

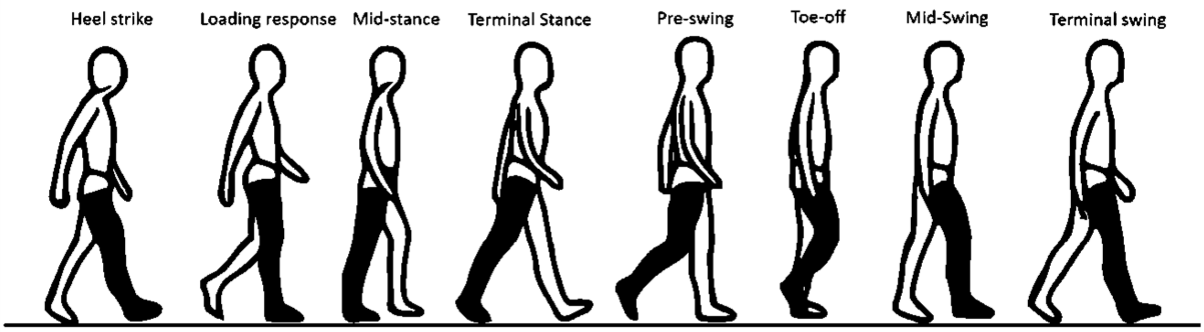

Figure 3: A healthy full gait cycle for one leg, spanning from initial contact (heel strike) through stance, swing, and back to the next heel strike. Adapted from CoachHackFeet [Internet] (43).

1.3 Balance

As stated before, OI allows for direct load transfer, minimizing soft tissue interference and therefore improving osseoperception relative to conventional socket-based prostheses (28). This improved sensory feedback in OIP may contribute to postural control, which primarily depends on the combination of sensory inputs such as proprioception, vision, and vestibular inputs (44). However, in individuals with a LLA, both proprioception and muscle contractions are affected due to the absence of a normal foot, ankle, knee, the surrounding muscles and ligaments, as well as affected stump muscles (45, 46).
A study by Rougier et al. (2009) found that both TTA-SP and TFA-SP patients develop compensatory strategies in the affected leg to maintain postural control, with TFA patients showing more pronounced strategies. This suggests that TFA-OIP patients, with enhanced osseoperception, may develop more effective mechanisms for postural control, leading to a more stable posture compared to TFA-SP patients. The increased feedback could help in refining these mechanism, potentially resulting in a posture more similar to non-amputees compared to TFA-SP patients (47).
However, up-to-date no clinically sensible biomarkers of gait and balance pathomechanics for comparison between OIP and SP above-the-knee prosthesis walkers have been established.

1.4 Study aim

The aim of this study is therefore to explore sensitive biomarkers of the altered gait biomechanics and balance control in people with an OIP versus people with a SP and versus non-amputees, conducted through a quantitative biomechanical analysis.

2. Methods

This was a cross-sectional and observational study. This study was classified as non-WMO research (i.e., not subject to the Dutch Medical Research Involving Human Subjects Act, WMO) by the local Medical Ethics Review Committee of the Erasmus Medical Centre, Rotterdam, the Netherlands (MEC-2021-0040, approval given on 03-02-2021). All procedures were conducted in accordance with the Declaration of Helsinki and all participants provided written informed consent.

2.1 Participants

This study included adult participants, which were divided into three research groups: healthy controls (HC), amputees with an OIP, amputees with an SP. The following sections describe the eligibility criteria for participation, as well as the recruitment procedures used to identify and enrol suitable participants

2.1.1 Inclusion- and exclusion criteria

Potential TFA participants were included if they had undergone an OIP-procedure or were potential candidates for an OIP while currently using a SP. Additionally, due to the nature of this research analysing the gait, participants were required to be able walk for a minimum of 2 minutes. Participants were excluded if they have balance disorders, neurological disorders (e.g. Parkinson's Disease or Multiple Sclerosis), or dependency on a walking aid (e.g. walking stick, walkers or relying on the railing). All inclusion- and exclusion criteria can be seen in Table 1.

Table 1: Inclusion- and exclusion criteria which participants need to meet to be eligible to participate in this study.

Inclusion Criteria		
Socket prosthesis (SP) group	**Osseointegrated prosthesis (OIP) group**	**Control group**
Age 18 years or older	Age 18 years or older	Age 18 years or older
Unilateral transfemoral amputation	Unilateral transfemoral amputation	
Using a socket prosthesis	Using an osseointegrated prosthesis	
Potential candidates for osseointegration	Finished full rehabilitation	
Able to walk for at least 2 minutes	Able to walk for at least 2 minutes	
Signed informed consent by patient	Signed informed consent by patient	Signed informed consent by patient
Exclusion Criteria		
Socket prosthesis (SP) group	**Osseointegrated prosthesis (OIP) group**	**Control group**
Any balance or neurological disorder	Any balance or neurological disorder	Any balance, neurological or movement disorder
Dependency on the use of walking aids during experiment	Dependency on the use of walking aids during experiment	Dependency on the use of walking aids during experiment
Insufficient Dutch language proficiency	Insufficient Dutch language proficiency	Insufficient Dutch language proficiency

2.1.2 Recruitment

Participants were recruited through clinical databases from two specialized centres in the Netherlands. Individuals in the OIP group were identified from the medical records of all patients who had undergone unilateral TFA followed by osseointegration surgery (TFA-OIP) at the Erasmus Medical Centre, Rotterdam, and were contacted by their treating surgeon. All included OIP participants were treated within this centre by a dedicated surgical team. The SP group was recruited from the Rijndam Rehabilitation Centre, Rotterdam, where patients with a unilateral transfemoral amputation using a SP were identified and contacted by their treating physician. Inclusion in the SP group required participants to experience substantial problems with socket use, making them potential candidates for future osseointegration. A third group consisted of able-bodied adults without a LLA or disorders impairing movement. Controls were primarily recruited by asking OIP and SP participants to bring a nondisabled friend or partner of similar demographic characteristics to serve as a control participant. If no suitable acquaintances were available, controls were recruited from hospital personnel with comparable demographic characteristics to the OIP and SP groups.

Each participant visited the Motion Biomechanics & Imaging (MOBI) Laboratory once. The measurements were conducted by the main researcher, with initial supervision and guidance from a more experienced researcher. This included calibration of the systems, as well as applying the motion capture markers and performing the measurement.

2.2 Measurements-protocol

The gait and balance analysis in this study aimed to assess and quantify the walking ability and stability parameters which are influenced in people walking with different types of prostheses. The gait analysis included spatiotemporal, kinematic, and kinetic parameters, which are crucial for understanding the mechanics of movement. Balance analysis examined differences in centre of pressure (CoP) length, range of motion and force distribution between the legs under three varying sensory and cognitive conditions. These measurements were used to provide insight into the participants stability and ability to maintain balance in different settings. The protocol to perform the measurements is outlined below in Table 2.

2.2.1 Familiarization

Prior to the calibration and measurements of the trial, participants walked on the treadmill for several minutes to become accustomed to the lab-environment and to establish a comfortable self-selected walking speed. The familiarization period was determined between the researcher and participant, based on verbal feedback, and observed comfort, due to physical fitness variations, particularly for individuals walking with a prosthesis, for whom energy demands are higher. This approach aimed to aligns with recommendations that of 5–10 minutes is sufficient for gait parameters to stabilize in healthy adults (48).

2.2.2 Calibration

After familiarization, two calibration trial were performed. First a static calibration trial, which is used for scaling in OpenSim, to meet each participant’s anthropometry (i.e., their body dimensions and proportions). Secondly, a dynamic calibration trial was performed to functionally determine joint centres and confirm marker tracking accuracy within VICON prior to data collection. After both calibration trials, within Vicon Nexus, reconstruction and labelling steps were performed to ensure correct labelling and reconstruction of segments.

2.2.3 Walking test

During dynamic calibration, participants were asked to walk at a comfortable, self-selected speed (SSS). Trials started with low speed and was gradually increased, with continuous verbal feedback between researcher and participant. The objective was to identify a walking speed representative of the participant’s natural, everyday speed. This speed was subsequently used to perform the measurement for the SSS. Subsequently, a second walking trial was performed at an imposed speed (IS) of 1 m/s (3.6 km/h) to allow comparisons across all participants. This speed was selected based on research by Vandenberg et al. (2024), in which SSS decreased from 1.07 m/s to 0.97 m/s after intervention for patients transitioning from SP to OIP. Therefore, 1 m/s was considered a feasible and representative speed for both SP and OIP patients (41).

2.2.4 Balance test

Balance control was assessed with static balance tests to investigate the stance stability. Each trial lasted 20 seconds and was performed under three conditions: Eyes open, Eyes Closed, and Eyes Closed with a Dual-Task. During the first and second trial, participants stood on the force plates, and the forces exerted by each leg were recorded to quantify balance performance and weight distribution between the legs. For the third balance trial, participants performed a cognitive task while maintaining balance, counting backward aloud from 100 in steps of 3. This task aimed to divert attention from balance to assess intuitive postural control.

Table 2: Overview of balance and gait measurements performed for each participant.

Measurement overview		
1	**Calibration trials**	
1.1	Static trial (standing still)	10 seconds
1.2	Dynamic trial (walking)	1 minute
2	**Gait trials**	
2.1	Self selected speed	2 minutes
2.2	Imposed walking speed (1 m/s)	2 minutes
3	**Balance trials (standing still on both legs)**	
3.1	Eyes Open	20 seconds
3.2	Eyes Closed	20 seconds
3.3	Eyes Closed with Dual-Task	20 seconds

2.3 Data collection

2.3.1 Experimental setup

Marker protocol: CGM 2.5

Passive reflective markers of 17 mm in diameter were used to track participant movement. The Conventional Gait Model (CGM), version 2.5, was used as the marker protocol (49, 50). The marker set was adjusted to fit the needs of this research, leading to 43 markers, where the markers on the arms were omitted, the T2-marker was repositioned to C7, and the T10-marker repositioned to T12. The markers can be categorized into two groups, anatomical markers and cluster markers. Anatomical markers are placed on palpable bony landmarks and are used for scaling and defining joint centres, while cluster markers are attached to segments and primarily used for tracking during dynamic trials. Marker locations on the participant are illustrated in Figure 4, and all marker location are described in Table 3.

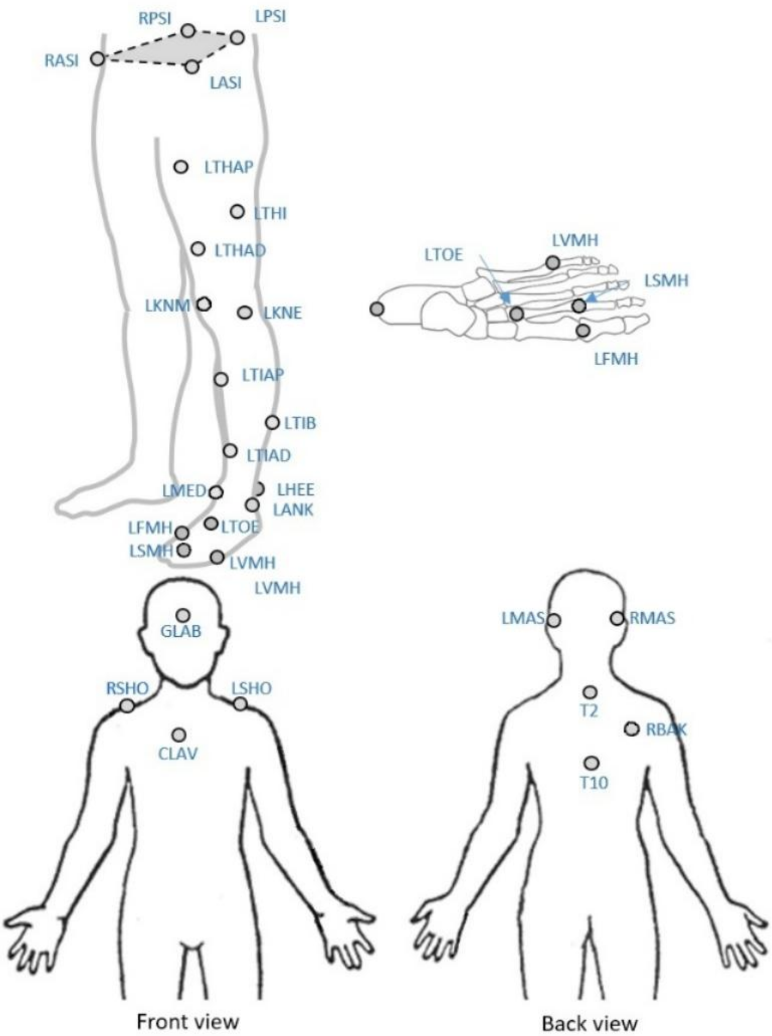

Figure 4: Illustration of the original marker placement according to the CGM 2.5, adapted from the CGM website (50). Marker labels and locations for the lower limb are shown unilaterally for clarity.

Table 3: Marker locations with abbreviations following the CGM version 2.5. Cluster markers are underlined in the abbreviations list, while anatomical markers are not.

Body part	Abbreviations	Explanation
Foot	LHEE/RHEE	Calcaneus at the insertion of the Achilles tendon
	LFMH/RFMH	1st metatarsophalangeal joint
	LSMH/RSMH	2nd metatarsophalangeal joint
	LVMH/RVMH	5th metatarsophalangeal joint
	LTOE/RTOE	2nd metatarsal-cuneiform joint
Tibia/Prosthesis	LANK/RANK	Lateral malleolus
	LMED/RMED	Medial malleolus
	LTIAP/RTIAP	Prominence on the superior anterior tibia
	LTIB/RTIB	Halfway down the lateral lower leg
	LTIAD/RTIAD	Halfway down the lower leg on the crest of the tibia
Femur/Prosthesis	LKNE/RKNE	Lateral epicondyle of the femur
	LKNM/RKNM	Medial epicondyle of the femur
	LTHI/RHTI	Halfway up the lateral thigh
	LTHAD/RTHAD	Distal anterior thigh
	LTHAP/RTHAP	Proximal anterior thigh
Pelvis	LASI/RASI	Iliac crest anteriorly
	LPSI/RPSI	Iliac crest posteriorly
Torso	LSHO/RSHO	Acromion
	C7	7^{th} cervical vertebra
	T12	12^{th} thoracal vertebra
	CLAV	Between the clavicles, above the sternum
	RBAK	Right back marker (technical marker for left-right orientation of the model)
Head	GLAB	Glabella (Between eyebrows, above nose)
	LMAS/RMAS	Mastoid process (Temporal bone)

MOBI-Lab

Figure 5: The MOBI-lab in in the Erasmus MC, Rotterdam, the Netherlands

All measurements were conducted in the MOBI-Lab within the Erasmus Medical Centre (EMC), Rotterdam, the Netherlands. The lab is equipped with the Motek M-Gait dual-belt treadmill, with integrated force plates, which is controlled through D-Flow software (51, 52). The motion capture system consists of 10 Vicon motion capture cameras which can detect the passive reflective markers on and around the treadmill (53), which is controlled using the Vicon Nexus Software (54). Ground reaction forces (GRF) were recorded at a sampling frequency of 1000 Hz, and marker data from the motion capture system were recorded at 100 Hz. Figure 5 shows the MOBI-Lab setup, including the treadmill, and motion capture system used for data collection.

Safety

To ensure participant safety, handrails were available for balance, and the treadmill could be stopped via the operating software, emergency buttons, or laser sensors at the front and back. Additionally, a ceiling-mounted safety harness was used to prevent falls (55). All safety measures and procedures in case of a fall were explained to participants prior to each measurement.

Data Export

After completing all five trials, the data were processed in Vicon Nexus. A 6 Hz Butterworth filter was applied to reduce measurement noise, and the processed data were exported as .c3d files, which contained both marker trajectories and force plate data for each trial.

2.4 Post-Processing Data

2.4.1 Musculoskeletal modelling

For musculoskeletal modelling and simulation, OpenSim version 4.5 was used during this study. OpenSim is open source, which is used for biomechanical modelling, simulation and analysis (56). It provides tools that allow researchers to create, scale, and analyse musculoskeletal models based on experimental data. In this study, OpenSim was used to process motion capture and GRF data. This included model scaling, inverse kinematics (IK), and inverse dynamics (ID) analyses (Figure 6).

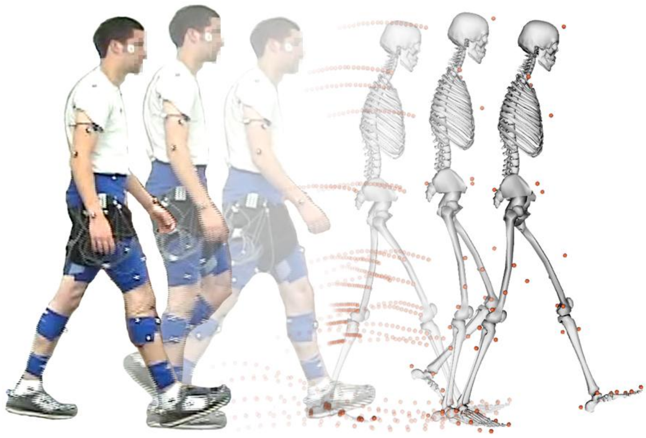

Figure 6: Inverse Kinematics Tool Overview. Experimental markers are matched to model markers for each frame in the captured motion adjusting joint angles, minimizing the overall error between experimental and virtual markers.

A total of 5 generic models were used: one for the healthy control group, and two each for the OIP and SP groups (left and right sides). An example of the generic models can be seen in Figure 7.

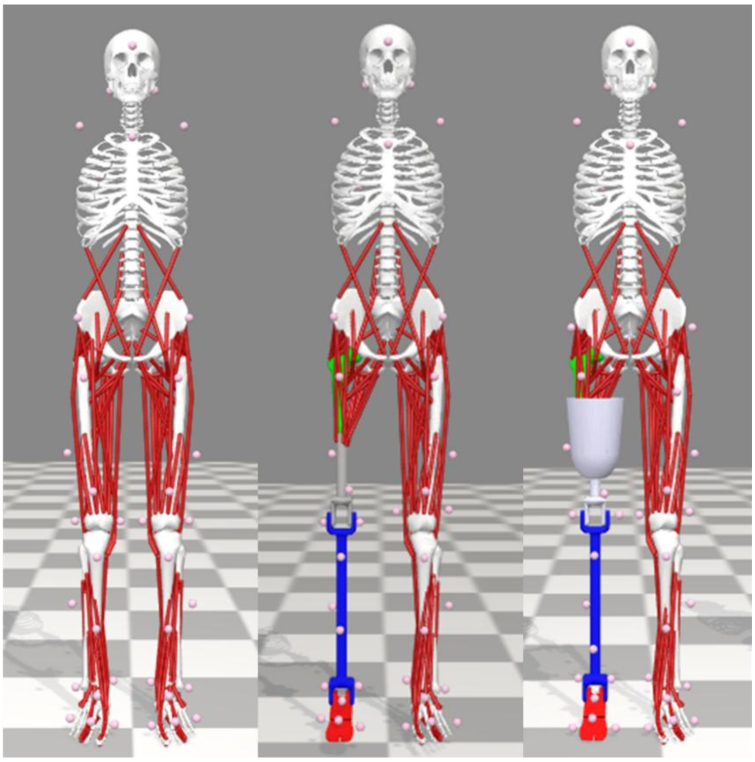

Figure 7: Biomechanical models used in this study, shown from left to right: healthy control, osseointegrated prosthesis (right leg), and socket prosthesis (right leg).

Healthy control model

For the healthy group, the base model Gait2392 was used, available from the OpenSim Documentation Wiki and developed by the OpenSim development team (57). The model has 23 degrees of freedom (DoFs) and features 92 musculotendon units to represent 76 muscles in the lower extremities and torso, with a standard height of 1.80 m tall and 75.16 kg.

Osseointegrated prosthesis models

For the OIP group, the Gait1976 model was used, which has been developed by Raveendranathen et al. (2020) (58). The generic model was available for both left- and right-sided amputees. The Gait1976 model was created by modifying the Gait2392 model, to create a generic musculoskeletal model of people with a unilateral transfemoral amputation wearing a generic OIP. The model consists of 19 DoFs and 76 musculotendon units. Of the 19 DoFs, 3 describe the torso (lumbar bending, extension, and rotation), 6 describe the pelvis (translation in the X, Y, and Z directions, and pelvic tilt, list, and rotation), 3 describe each hip joint (flexion, adduction, and rotation), 1 describes each knee joint (flexion), and 1 describes each ankle joint (dorsiflexion and plantarflexion).

Socket prosthesis models

For the SP model, the OIP model (Gait1976) was modified by removing the OI pylon in OpenSim. The socket structure from a TTA-SP model, together with its associated DoFs (flexion, adduction, rotation, and pistoning along the y-axis, translations along the x- and z-axes were locked), was adapted and connected to the transfemoral segment (59). To fit the socket to the transfemoral model, the socket size was increased, and the socket component from the TTA-SP model was joined with the OIP pin segment from the OIP model, attaching the socket to the residual femur component. The components were merged using Blender (version 3.2.2) (60), and the weight of the new socket assembly was recalculated based on the known weights of the individual parts. This allowed for reuse of the remaining tibia and foot components of the prosthetic leg, by being able to connect the tibia and foot parts to the femur part. This reduced structural differences between the SP and OIP models, aiming to facilitate similarity between models, instead of using a new model.

In all models, an additional DoF was added to the knee joint to represent knee adduction, in addition to the standard knee flexion–extension. This DoF was locked at 0°, so it did not affect the model's kinematic outcomes, however it allowed calculation of the knee adduction moment (KAM) using ID. It needs to be noted that in all models, the two DoF's of the feet (subtalar and metatarsophalangeal (MTP) joints) were locked for to enable direct comparison between feet and the different subjects. This was done to simplify the foot dynamics, as the prosthesis feet are a simplified version of a real foot. In the models within OpenSim, the model does not incorporate shoes. Due to safety reasons, participants were required to wear shoes.

2.4.2 Processing pipeline

The method to process the collected data within OpenSim, is outlined in the following sections. A general overview of this process is illustrated in the flowchart in Figure 8.

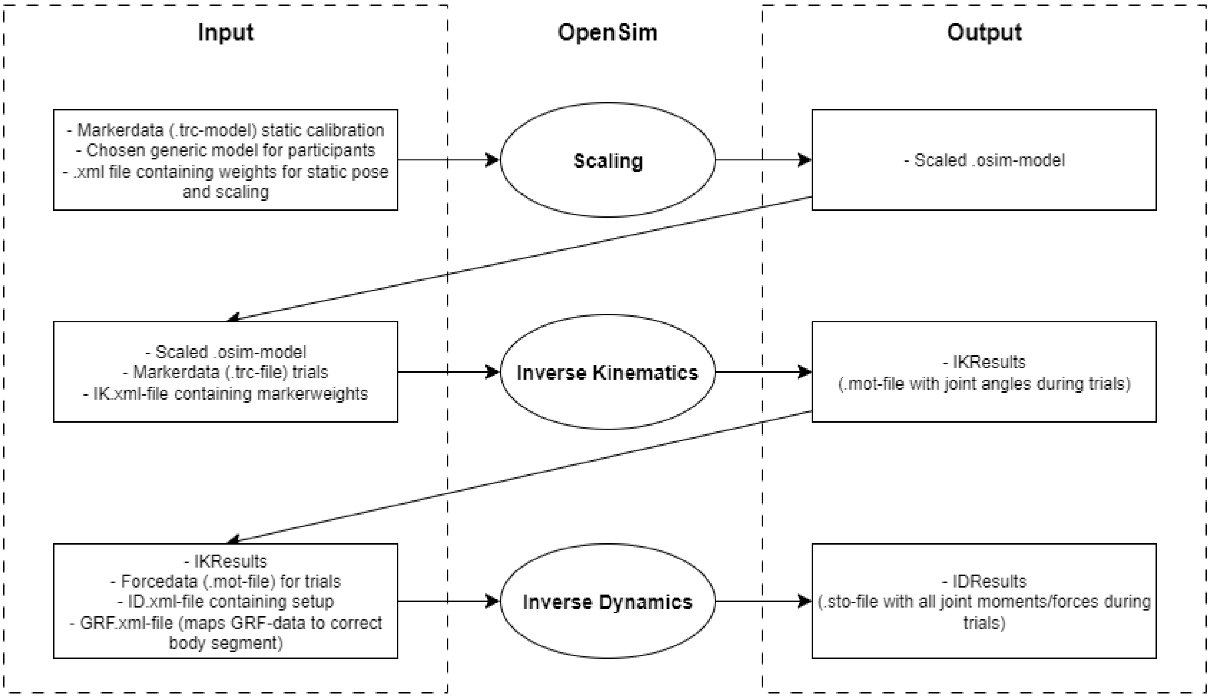

Figure 8: Flowchart illustrating of analysis in OpenSim, including scaling of the generic model, inverse kinematics for joint positioning, and inverse dynamics for calculating joint forces and moments.

OpenSim Scaling

After measurements, the appropriate generic .osim- model was chosen for each participant. The .osim- model was scaled in OpenSim using the Scale Tool, and based on a static calibration trial recorded at the start of each measurement session (56). The Scale Tool adjusts the generic model's segment dimensions to match the participant's anthropometry by aligning virtual model markers with experimental marker positions from the static trial, producing a subject-specific model for subsequent analyses. Afterwards, the scaled model is used as input for the processing in IK and ID to calculate the parameters of interest for each participant and group totals.

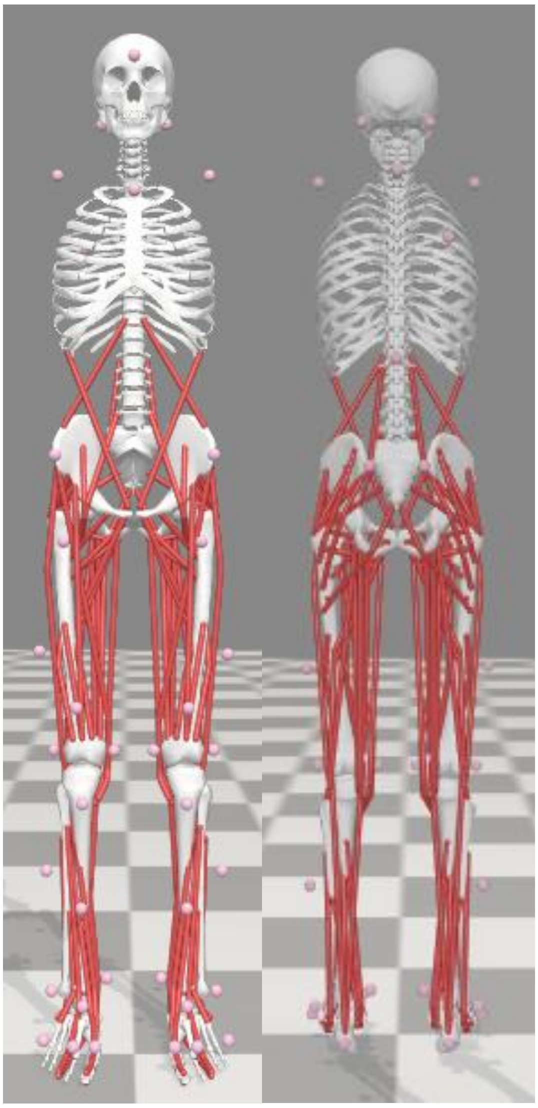

Figure 9: Anterior and posterior view of markers (pink) as placed on the generic model used for the healthy/control group.

Inverse Kinematics

The IK Tool processes each recorded frame by positioning the model's joints and rigid bodies to minimise the mean weighted error between the experimental marker data and corresponding model markers. The joint angles which define the resulting positions are saved and can be used in other tools.

Inverse Dynamics

The ID Tool calculates the net forces and torques at each joint required to produce a specific movement in the joint. It uses the IK results and GRF, which was captured by the force plates). The ID tool applies the principles of classical mechanics in a reverse manner, working from motion back to force. By solving the equations of motion inversely, the ID Tool determines the joint-level forces and torques necessary to produce the observed movement within each frame.

Python scripts for IK, ID, and processing

Partially existing scripts, developed by previous researchers, were adapted and extended with custom Python scripts to automate and streamline the data processing and statistics pipeline. These scripts managed tasks such as converting raw motion capture data (.c3d) into OpenSim-compatible formats such as .trc- (marker data, 100Hz) and .mot-files (force data, 1000 Hz) and performing IK and ID analyses for all participants. Additional scripts were used to process outcomes such as spatiotemporal gait parameters, extract peak vertical GRF (vGRF) and analyse balance data using CoP metrics. All scripts were modular, relying on shared functions and metadata extracted from Excel files. A full overview of the scripts and their functions is provided in Appendix A1, and a flowchart illustrating their interconnections is provided in Appendix A2.

2.4.1 Gait measures

Spatiotemporal parameters

Spatiotemporal gait parameters were extracted from marker (.trc) and force (.mot) files, for both the SSS and IS. Gait events, specifically heel strike and toe-off, were identified based on the recorded vGRF. In combination with treadmill belt speed, parameters were calculated for each complete step and reported as mean ± SD across all valid steps per leg.

- Stance and swing time: Defined from heel strike to toe-off (stance) and toe-off to subsequent heel strike (swing).
- Stride time: Calculated as the sum of stance and swing phase and averaged across all full strides.
- Cadence: Calculated as $120/\text{mean stride time}$. Direct step counting was avoided, since in the dual-belt treadmill setup steps were occasionally mis-registered when a foot landed across the opposite belt, preventing consistent counts.
- Step length: Step length was calculated as $\text{treadmill speed} \times \text{step time}$, where step time was the interval between contralateral heel strikes. Step length was only calculated when a contralateral step could be clearly identified, meaning when the heel strike of one foot occurred within the stance phase of the opposite leg.

Joint Kinematics & Trunk Lean

To perform IK, the OpenSim Python packages were used to automate processing. After scaling, the models were run through IK. From the IK analysis, the following joint kinematics were extracted (in degrees): hip flexion, hip adduction, hip rotation, knee flexion, and ankle flexion. Lateral trunk lean was included as an extra measure, as the models used in OpenSim focus on lower-limb biomechanics.

Lateral trunk lean in the coronal plane was defined as the angle between the vertical axis and the trunk axis. The vertical axis was defined as the sagittal plane when seen from a posterior view. The trunk axis was defined as the line passing through marker C7 and a point approximating the sacrum, calculated as the midpoint of the left and right posterior superior iliac spine (LPSI and RPSI) markers. A similar approach has been described in a study performed by Tokuda et al. (2017), where the trunk axis was defined using the midpoints of the PSIS and acromion markers (61). Within this study, C7 was used instead of the acromion midpoint, to capture upper spinal alignment more directly. In Figure 10, the points used for calculation and the lateral trunk lean angle is illustrated (62).

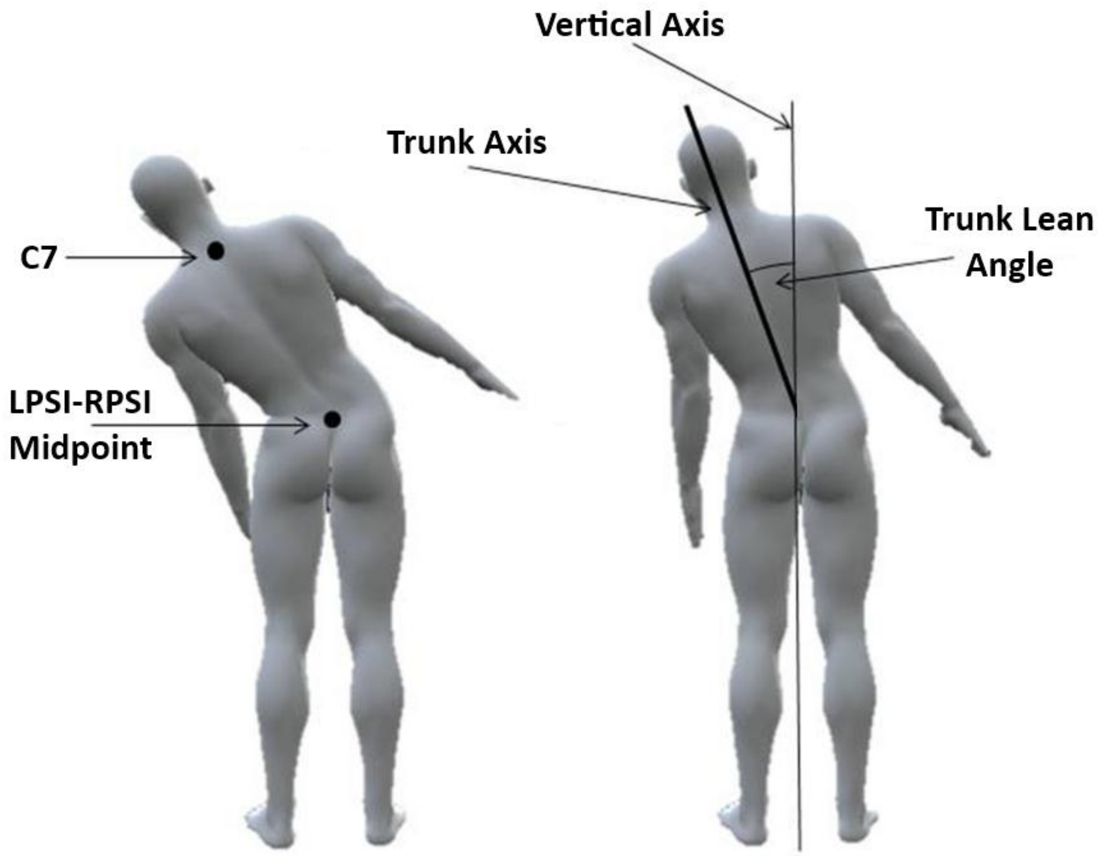

Figure 10: Illustration of the Trunk Lean Angle, defined as the Angle between the Vertical Axis and the Trunk axis. Adapted from Mikami et al. (2022), with modifications (62).

Joint Kinetics

As with IK processing, Python packages were used to automate ID processing. Joint moments were calculated for the joints which were processed with IK, with addition of the knee adduction moment. The extracted kinetics were hip flexion moment, hip adduction moment, hip rotation moment, knee flexion moment, knee adduction moment and ankle flexion moment, all in Nm/kg.

Margin of Stability

Just as in static stability, where the Centre of Mass (CoM) needs to be within the Base of Support (BoS), the legs need to create a BoS during gait for the moving body. To measure the balance during gait, the Margin of Stability (MoS) extends the concept of static stability to dynamic stability by accounting for momentum, allowing an individual to be stable even with their CoM lies outside of the BoS.
A larger MoS indicates that the body's projected motion remains safely within the support area, whereas a smaller or negative MoS suggests a greater risk of instability or loss of balance (63, 64). The MoS can be calculated with the following formula:

$$MoS = BoS - X_{CoM} \ (Equation\ 1)$$

To account for the velocity, the velocity-adjusted position of the CoM is calculated, or extrapolated CoM (XCoM), was calculated as:

$$X_{CoM} = CoM + \frac{v}{\omega_0} \ (Equation\ 2)$$

where v is the velocity in the anteroposterior (AP) and in the mediolateral (ML) direction, and $\omega 0$ is the eigenfrequency of the inverted pendulum of the body:

$$\omega_0 = \sqrt{\frac{g}{l}} \ (Equation\ 3)$$

In this formula, g = 9.81 m/s2 is the gravitational acceleration and l as the pendulum length, defined as the three-dimensional distance between the CoM and the heel marker at heel strike.

By incorporating both position and velocity of the CoM relative to the supporting foot, the MoS provides a dynamic assessment of gait stability beyond static measures of balance. This makes it particularly relevant for comparing populations with potentially impaired stability, such as individuals with lower-limb prostheses, to HC.

Based on a study performed by Dussault-Picard et al. (2025), the most anterior marker should be used to define the BoS in the AP direction, while the HEE should be used for ML direction, as these markers provide the closest agreement with CoP-based measures of the MoS (65). For the present calculations, the SMH marker was used

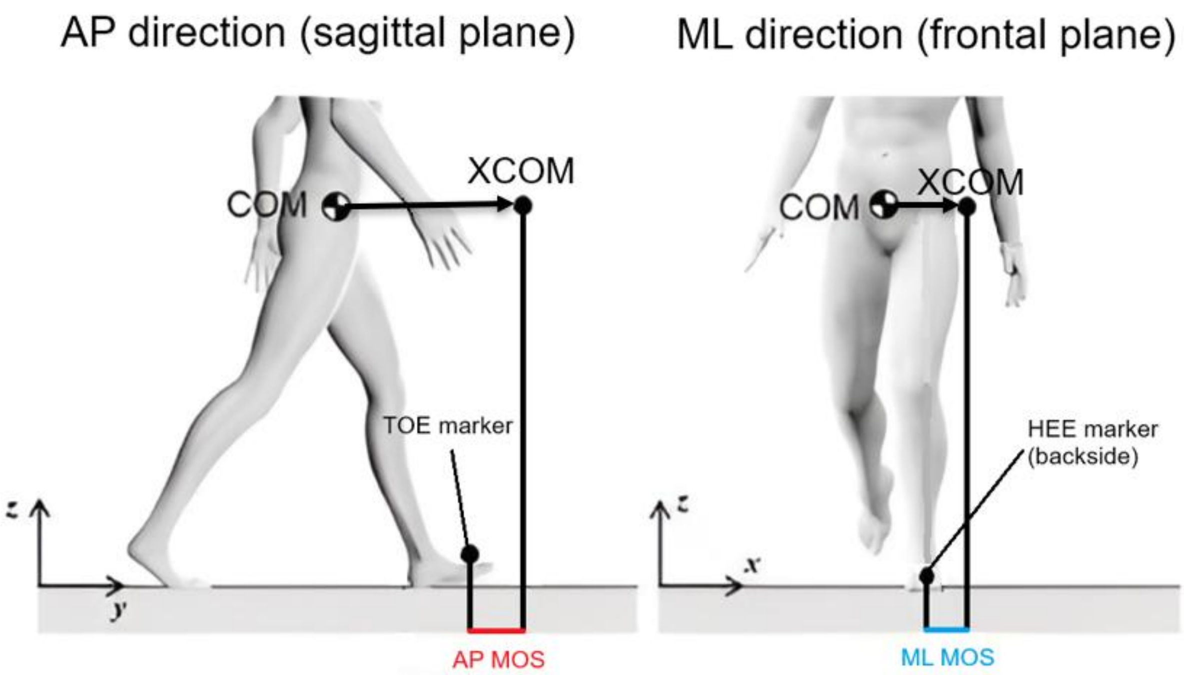

Figure 11: Schematic of the Margin of Stability for AP and ML. For the ML MoS, the HEE marker is positioned at the back of the foot but is illustrated from an anterior viewpoint for visualization purposes. Adapted from Yamaguchi and Masani (2022), with modifications (66).

to define the BoS in the AP direction, as this is the most anterior marker placed on participants. For the ML direction, the HEE marker was used. The CoM was approximated as the average of the four pelvic markers (LASI, RASI, LPSI, and RPSI). As shown in Figure 11, the MoS is illustrated in both AP and ML directions, along with the CoM and XCoM displacement (66). MoS was calculated separately in the AP and ML directions for both legs. For the AP direction, the MoS at heel strike was calculated for each step and then averaged across all steps per leg. For the ML direction, the MoS was calculated throughout the entire stance phase of each step, and the minimum value per step was identified. These minimum ML values were then averaged across all steps per leg.

2.4.2 Balance parameters

Centre of pressure (CoP)

The balance trials were processed from the forces-files, which contained the GRF data (three XYZ-force components, three XYZ-centre-of-pressure coordinates, and three XYZ-moments). From these components, CoP-metrics such as path length and ROM in the AP and ML direction were consistently mapped to the NA and affected sides based on patient metadata, and results were summarized per condition, including both individual and group (mean ± SD) values.

Loading distribution and Symmetry Index

To assess differences in loading between the legs, symmetry was evaluated using the relative loading per leg (NA and affected as a percentage of total measured GRF in the trial) and a mean-based Symmetry Index (SI).
In a study performed by Błażkiewicz et al.(2014), which compared four different symmetry metrics including the Ratio Index, the SI was identified as the most sensitive and diagnostically useful measure, offering advantages over other metrics (67). The SI expresses asymmetry between legs as a single metric, which allows for group-level comparisons (67). At the same time, a ratio of relative loading percentages remains useful for clinical interpretation, due to their intuitive interpretation. Therefore, both metrics are reported in the results to provide a complete overview.

For each 20-second trial, the mean vGRF values of each leg were used to calculate the SI (Eq. [4]). To preserve the positive-negative interpretation, the force of the non-affected leg (X_{NA}), and the force of the affected leg (X_A) were defined such that a positive SI values indicates greater loading on the NA leg, while negative SI values indicate greater loading on the affected leg. Group-level mean ± SD SI values enabled straightforward comparison between groups, although this approach reduces within-trial temporal detail (68). Table 4 presents the classification of SI values.

$$SI = \frac{(X_{NA} - X_A)}{0.5 \times (X_{NA} + X_A)} \times 100\% \ (Equation\ 4)$$

Table 2: Classification of Symmetry Index (SI) values: ±10 = near symmetry, ±10–20 = moderate asymmetry, >±20 = high asymmetry. (68)

Symmetry Index	Interpretation
Perfect (0)	Perfect symmetry: both legs exert the same force.
Low (±10)	Nearly symmetric. Mild asymmetry.
Moderate (±10–20)	Slight imbalance, potentially compensatory.
High (>±20)	Significant asymmetry, often due to pathology or compensation.

3. Results

3.1 Demographics

In total, 13 participants were included in this study. Of these 13, five were healthy individuals, five had an OIP and three had an SP. Within the prosthesis groups, all participants were fitted with a MPK combined with a carbon fibre prosthetic foot. The OIP group was older than the HC (67.2 ± 4.8 vs 57.4 ± 16.0 years), while the SP group was similar in age compared to HC (59.7 ± 13.5 years). SP participants were taller and heavier, yielding the highest BMI (29.9 ± 4.9) compared with OIP (26.7 ± 4.3) and controls (23.9 ± 0.9). Daily prosthesis wear time was higher in OIP than SP (16.4 ± 0.9 vs 13.3 ± 2.3 h/day). It should be noted that the SP group comprised only males, which, together with BMI differences, should be considered as potential confounders. All characteristics of participants and group information can be seen in Table 5.

Table 3: Demographic and clinical characteristics of the patient cohort, including age (years), height (cm), weight (kg), body-mass index (kg/m²), years since amputation, average prosthesis usage per day (hours), and self-selected walking speed (m/s).

Patient ID	Sex (M/F)	Age (Years)	Height (Cm)	Weight (Kg)	BMI (Kg/m²)	Affected leg	Years since amputation	Prosthesis usage per day (hours)
Healthy control group (HC)								
HC mean	**-**	**57.4±16.0**	**179.5±11.4**	**76.9±7.6**	**23.9±0.9**	**-**	**-**	**-**
Participant 1	Male	68	191	83	22.8	-	-	-
Participant 2	Female	73	170	72.5	25.1	-	-	-
Participant 3	Female	54	165.5	65.8	24	-	-	-
Participant 4	Female	60	181.5	79.8	24.2	-	-	-
Participant 5	Male	32	189.5	83.5	23.3	-	-	-
Osseointegrated prosthesis group (OIP)								
OIP mean	**-**	**67.2±4.8**	**173.6±8.5**	**80.8±17.5**	**26.7±4.3**	**-**	**25.8±17.0**	**16.4±0.9**
Participant 1	Male	71	181	87.2	26.6	Left	52	16
Participant 2	Male	70	182.5	107.8	32.4	Left	31	16
Participant 3	Female	68	167	70.8	25.4	Right	24	16
Participant 7	Female	59	174.5	62.7	20.6	Right	12	18
Participant 8	Female	68	163	75.9	28.6	Left	10	16
Socket prosthesis group (SP)								
SP mean	**-**	**59.7±13.5**	**186.6±6.0**	**104.9±24.3**	**29.9±4.9**	**-**	**21.6±15.9**	**13.3±2.3**
Participant 2	Male	73	193	132.6	35.6	Right	14	12
Participant 6	Male	60	186	94.7	27.4	Left	11	16
Participant 8	Male	46	181	87.4	26.7	Left	40	12

3.2 Gait

3.2.1 Spatiotemporal parameters

Spatiotemporal gait parameters are summarized in Tables 6 and 7 for both IS (1 m/s) and SSS. At the IS, cadence was highest in HC (109.7 ± 19.9 steps/min) and lowest in the SP group (87.9 ± 10.4), with OIP participants in between (101.9 ± 9.4). Due to their lower cadence, OIP and SP participants compensated with longer steps, particularly with the affected leg (0.64 m in OIP and 0.70 m in SP) compared to controls (0.56 m), allowing them to maintain the speed. In both prosthesis groups, for the stance-to-swing ratios there is asymmetry, with OIP participants showing longer stance on the NA leg (67/33) compared to the affected leg (60/40), and SP participants showing a slightly greater difference between the legs (69/31 vs. 61/39).

Table 4: Spatiotemporal gait parameters at imposed walking speed (1 m/s). Values are reported as group means ± standard deviation (SD) or as stance/swing ratios (% of total).

Spatiotemporal parameters: Imposed speed (1 m/s)	**Groups**		
Parameters per avg. step (Mean ± SD)	**HC**	**OIP**	**SP**
Overall			
Cadence [steps/min]	109.7 ± 19.9	101.9 ± 9.4	87.9 ± 10.4
Non-affected leg			
Stance/Swing ratio [%]	64/36	67/33	69/31
Stride Time [s]	1.12 ± 0.16	1.18 ± 0.10	1.31 ± 0.14
Step Length [m]	0.55 ± 0.09	0.55 ± 0.05	0.61 ± 0.09
Affected leg			
Stance/Swing ratio [%]	64/36	60/40	61/39
Stride Time [s]	1.12 ± 0.16	1.18 ± 0.10	1.31 ± 0.14
Step Length [m]	0.56 ± 0.09	0.64 ± 0.06	0.70 ± 0.08

Asymmetry is seen in step length between the NA and affected leg in OIP and SP, with are relative larger asymmetry in the OIP, due to relative shorter steps. The NA leg in OIP users has a similar step length compared to the controls.

Table 7 shows the outcomes for SSS, where HC walked faster (1.13 ± 0.3 m/s) than prosthesis users (OIP: 0.98 ± 0.2 m/s; SP: 0.97 ± 0.3 m/s). As in the IS trials, cadence and stride duration differed between groups, with controls showing higher cadence (113.8 ± 12.5 steps/min) and shorter stride times (1.07 ± 0.11 s) compared to SP (88.7 ± 16.9; 1.36 ± 0.26 s). Step lengths were larger in SP participants (0.57-0.68 m), while OIP users (0.54-0.61 m) and controls (0.60-0.61 m) were similar in size. For the stance-to-swing ratio, participants of both groups had a longer stance on the NA leg (67/33) compared to the affected leg (61/39), while SP participants displayed a similar asymmetry. between legs (69/31 vs. 63/37).

Asymmetry is seen in step length between the NA and affected leg in OIP and SP, with a relative larger asymmetry in the SP users. This contrasts with the IS trials, where step lengths were slightly more asymmetrical in the OIP.

Table 5: Spatiotemporal gait parameters at self-selected walking speed. Values are reported as group means ± standard deviation (SD) as stance/swing ratios (% of total).

Spatiotemporal parameters: Self -selected speed	**Groups**		
Parameters per avg. step (Mean ± SD)	**HC**	**OIP**	**SP**
Overall			
Cadence	113.8 ± 12.5	100.3 ± 13.1	88.7 ± 16.9
Self-selected speed (m/s)	1.13 ± 0.3	0.98 ± 0.2	0.97 ± 0.3
Non-affected leg			
Stance/Swing ratio (%)	64/36	67/33	69/31
Stride Time (s)	1.07 ± 0.11	1.21 ± 0.15	1.36 ± 0.26
Step Length (m)	0.60 ± 0.16	0.54 ± 0.06	0.57 ± 0.09
Affected leg			
Stance/Swing ratio (%)	64/36	61/39	63/37
Stride Time (s)	1.07 ± 0.11	1.21 ± 0.15	1.36 ± 0.26
Step Length (m)	0.61 ± 0.16	0.62 ± 0.06	0.68 ± 0.10

Comparison of the two trial speeds showed that HC walked faster at SSS than prosthesis users, mainly through higher cadence In contrast, SP participants displayed lower cadence but consistently had longer step lengths than OIP users and controls. Stance-to-swing ratio asymmetries in the prosthesis groups were present under both walking trials.

3.2.2 Joint Kinematics

Kinematic and kinetic gait cycle data were analysed for both the IS and SSS conditions. As the SSS reflects the natural walking behaviour of each participant, within the results section, only the figures for these trials are shown. Corresponding plots for the IS trials are provided in the Appendix (B1-B4).

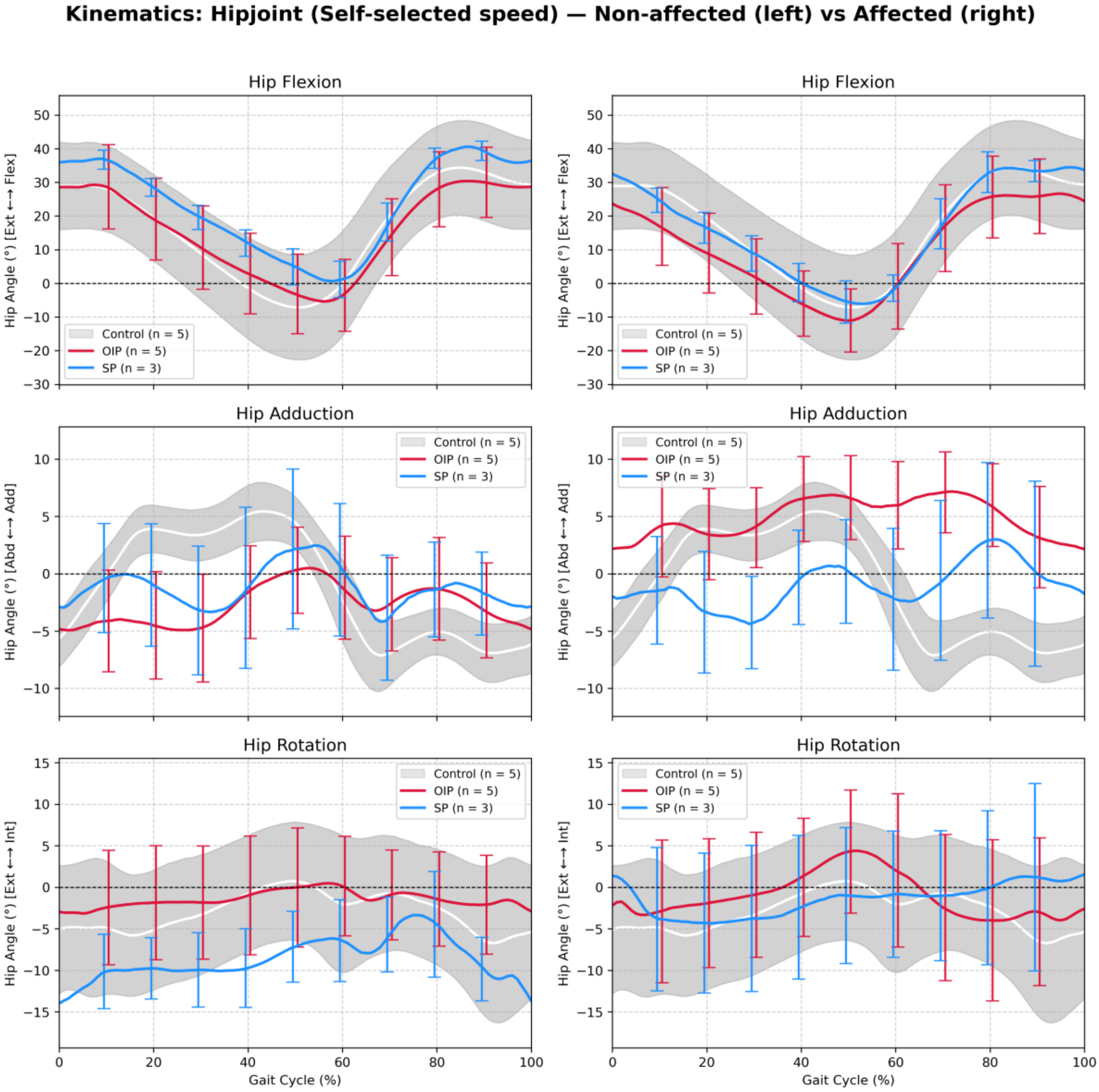

Figure 12: Hip joint kinematics at self-selected speed for healthy controls (grey, n = 5), OIP users (red, n = 5), and SP users (blue, n = 3). Left: non-affected side; Right: affected side. Rows show hip flexion/extension, adduction/abduction, and internal/external rotation across the gait cycle.

The kinematic outcomes for the hip for both the affected and NA legs across the three groups are shown in Figure 12. For hip flexion/extension, the control group shows the largest range of motion on both sides, with a distinct extension peak during terminal stance as the leg prepares for push-off. OIP users display a similar pattern on the NA side but with a delayed extension peak, while SP users show about 10 degrees more flexion during the first 60% and last 20% of the gait cycle compared to controls. For hip adduction, both OIP and SP users exhibit asymmetry between legs. For the NA leg in the prosthesis groups, the curve is roughly the same. But looking into the affected leg, OIP shows its entire curve in the adduction zone, while SP primarily abducting more. For both legs in the prosthesis groups, the hip adduction is quite different compared to HC.

For hip rotation, both the control and OIP groups show similar trends between the NA and affected sides, with internal rotation angles increasing for the OIP curve halfway the gait cycle.
For the affected leg in SP users the HC-curve is followed, in contrast to NA leg, which has a higher external rotation for the entire gait cycle.

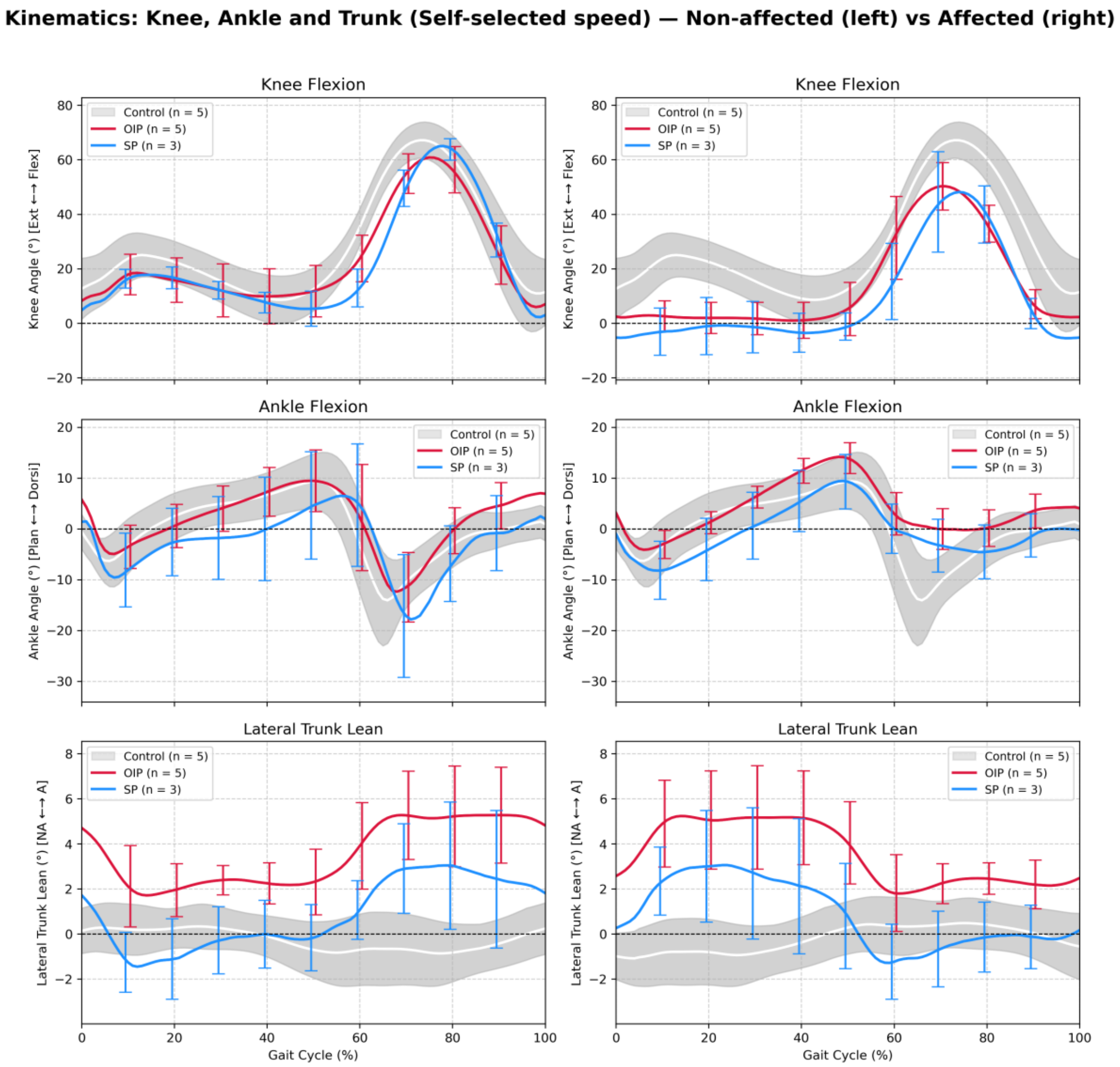

Figure 13: Knee, ankle and trunk kinematics at self-selected speed for healthy controls (grey, n = 5), OIP users (red, n = 5), and SP users (blue, n = 3). Left: non-affected side; Right: affected side. Rows show knee flexion/extension, ankle dorsi-/plantarflexion, and lateral trunk lean. ***Note****: For the lateral trunk lean, the data represents a single kinematic value for the entire trunk. Therefore, the same mean value is plotted for both the affected and non-affected sides, but with a shift. Positive values indicate leaning towards the affected side (A).*

The kinematic outcomes for knee, ankle, and trunk lean for both the affected and NA legs across the three groups are shown in Figure 13. In knee flexion, the HC, OIP and SP groups have a similar curve for the NA leg, with slightly lower flexion values in the prosthesis groups, with clear flexion peaks at initial swing phase (≈70% of gait cycle). In the affected leg, both prosthesis groups show lack of the flexion peak during the loading phase (≈10% of gait cycle), with OIP users showing a broader peak at initial swing compared to SP users. For ankle flexion, OIP users followed the HC-group on the NA side, but on the affected side, there was a slightly increased dorsiflexion and absence of the plantarflexion peak. SP users exhibited less dorsiflexion and more plantarflexion during stance on the affected side. Regarding lateral trunk lean, the control group showed a symmetric pattern with minimal deviation around 0 degrees, as is expected of HC. Both OIP and SP groups displayed greater asymmetry, with the OIP group, on average, bending more laterally toward the prosthetic side during gait. Although, for both groups, a relatively large spread of individual values is seen, especially during the stance phase.

3.2.3 Joint Kinetics

The kinetic outcomes for hip moments for both the affected and NA legs across the three groups are shown in Figure 14.

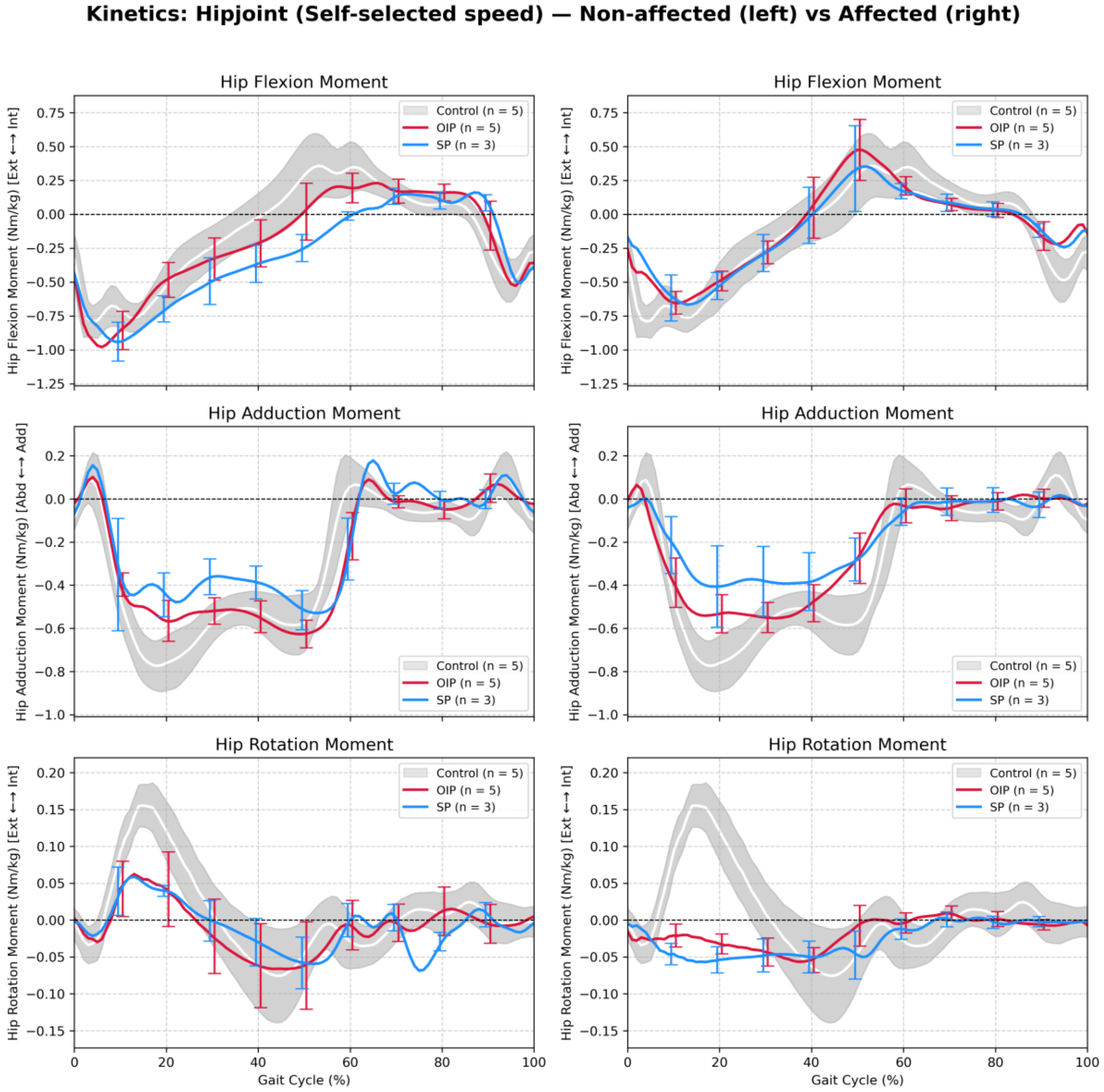

Figure 14: Hip joint kinetics at self-selected speed for controls (grey, n = 5), OIP (red, n = 5), and SP (blue, n = 3). Left: non-affected; Right: affected. Rows show hip flexion, adduction, and rotation moments across the gait cycle.

In the NA leg, both the OIP and SP groups show a trend like the HC group, with the HC group displaying a double peak during the terminal stance phase (≈50-60% of the gait cycle). However, the prosthesis groups show lower peak flexion moment values compared to controls, while all groups have a pronounced extension moment peak at the start/end of the gait cycle.

In the affected leg, both prosthetic groups show a reduced extension peak during the mid-stance phase (≈10% of the gait cycle). While at the terminal stance phase, the hip flexion peak is like the HC group for the prosthesis groups. At terminal swing, both prosthesis groups have a lower extension moment peak than the HC group.

For the hip adduction moment, in the NA legs all groups demonstrate a similar adduction pattern, although the prosthesis groups show slightly lower abduction values around mid-stance (≈20% of the gait cycle) compared to both control and SP groups.

On the affected leg, OIP and SP users display a similar curve as their counterparts in the NA leg, although with less pronounced peaks.

In hip rotation moment, the prosthesis groups exhibit similar behaviour in the NA leg from 30%, following the curve, but with a lower internal rotation peak than to the control group. In the affected leg, however, there are notable differences, with both prosthesis groups showing a lower external rotation peak, instead of a high internal peak.

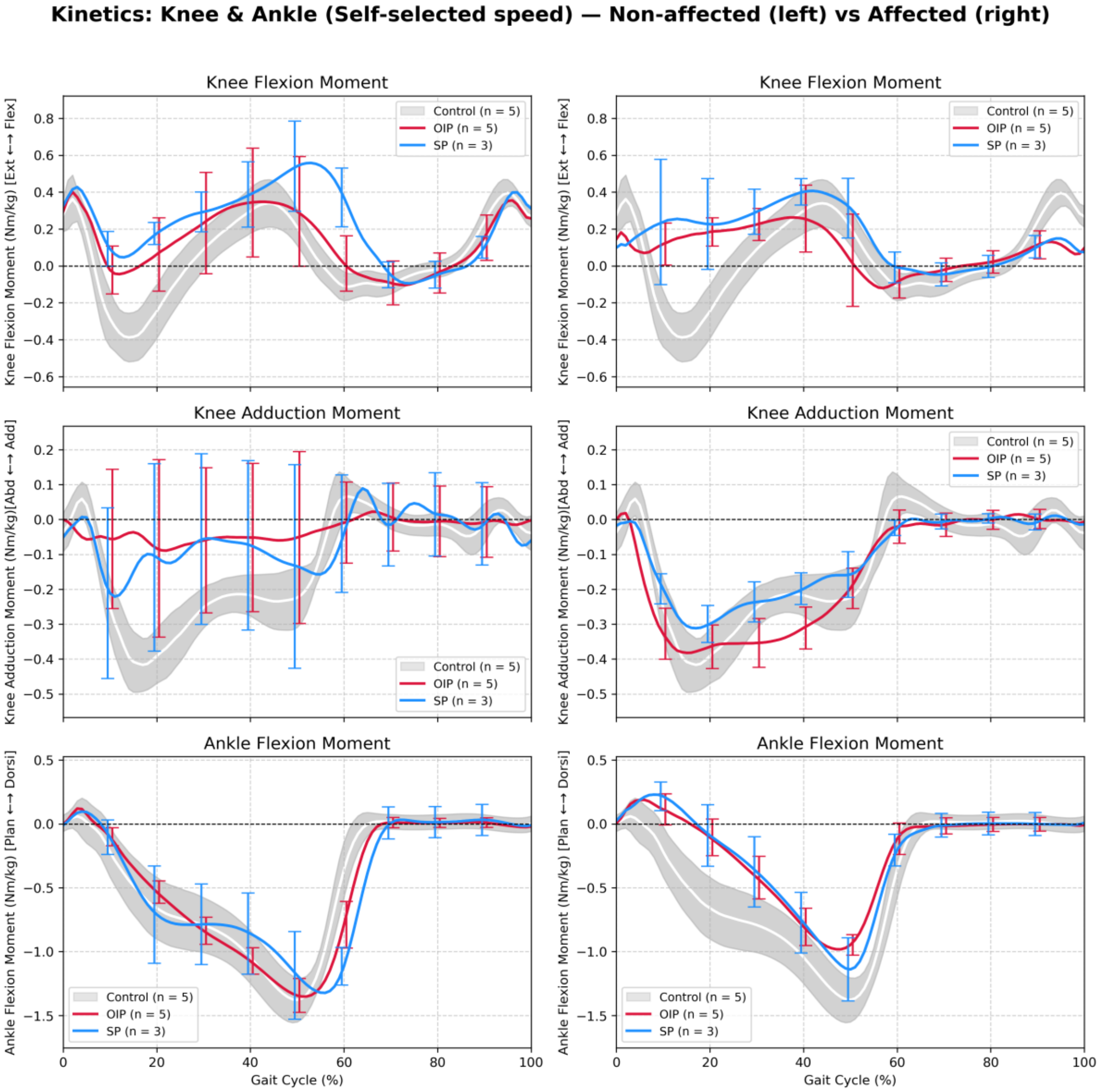

Figure 15: Knee and ankle joint kinetics at self-selected speed for controls (grey, n = 5), OIP (red, n = 5), and SP (blue, n = 3). Left: non-affected; Right: affected. Rows show knee flexion, knee adduction, and ankle flexion moments across the gait cycle.

The kinetic outcomes for knee and ankle moments for both the affected and NA legs across the three groups are shown in Figure 15. The knee flexion moment curves in the NA leg of the prosthesis group roughly follow the HC patterns, although with a lower extension moment peak value. For the affected leg, the prosthesis group only exhibited the same behaviour after 50%, so primarily in swing phase, where in stance it there is no clear pattern. For the knee adduction moment in the NA leg, during stance phase, the SP shows peak, whereas the OIP does not. Comparing the different curves is difficult due to large deviations between patients. For the affected legs, both prostheses groups follow the HC curves, only showing less high peaks, such as the HC group abduction peak at 20% and the slight adduction peak at 60%.

For the ankle flexion moment, the NA legs in all groups show similar behaviour, with only the SP group demonstrating a slight delayed extension peak, due to its prolonged stance phase. For the affected legs, the OIP and SP are similar, with both an offset of 0.5 Nm/kg less extension for the curve up to 50% of the gait cycle, whereafter they follow the HC group.

3.2.4 Margin of Stability

Table 6: Margin of stability (MoS) outcomes for both the non-affected and affected legs in the anteroposterior (AP) and mediolateral (ML) directions during imposed speed (1 m/s) and self-selected speed walking for HC, OIP, and SP groups. Values are presented as Mean ± SD.

Margin of stability	**Imposed speed (1 m/s)**			**Self-Selected speed**		
Groups	**HC**	**OIP**	**SP**	**HC**	**OIP**	**SP**
Non-affected leg outcomes (Mean ± SD)						
MoS AP (m)	0.37 ± 0.04	0.39 ± 0.08	0.41 ± 0.06	0.37 ± 0.07	0.38 ± 0.03	0.41 ± 0.03
MoS ML (m)	0.03 ± 0.06	0.01 ± 0.08	-0.03 ± 0.06	0.04 ± 0.06	0.02 ± 0.06	-0.02 ± 0.06
Affected leg outcomes (Mean ± SD)						
MoS AP (m)	0.36 ± 0.05	0.37 ± 0.03	0.37 ± 0.04	0.36 ± 0.07	0.37 ± 0.03	0.38 ± 0.05
MoS ML (m)	0.03 ± 0.06	0.05 ± 0.04	-0.02 ± 0.07	0.03 ± 0.05	0.06 ± 0.04	-0.02 ± 0.07

The MoS outcomes for both the affected and NA legs across the three groups during IS and SSS walking are presented in Table 8.

In the AP direction, the MoS for the NA leg showed similar values across all groups for both walking conditions, with no major differences in MoS observed between HC, OIP, and SP. The values ranged from 0.37 to 0.41m, with small variations between groups. For the affected leg, MoS values were also consistent across the groups, ranging from 0.36 to 0.38m in the AP direction, indicating similar stability across all conditions.

In the ML direction, the NA leg demonstrated similar stability across the groups in both walking conditions, with HC and OIP showing positive MoS values, while SP exhibited slightly negative values, indicating reduced stability. Negative values means that there is a lateral movement of the XCoM past the HEE marker, possibly moving outside the BoS. For the affected leg, the MoS in the ML direction was negative in SP group, suggesting a greater risk of instability or balance loss. For the OIP, there is a lower MoS compared to the HC in the NA leg, but higher MoS in the affected leg. This shows that the affected leg is placed more laterally to gain stability during gait. These values were consistent across both the IS and SSS conditions, indicating that the observed instability was not dependent on walking speed.

3.3 Balance parameters

3.3.1 Centre of Pressure

Table 9 shows the CoP outcomes for the NA and affected legs for the balance trials.

Table 7: Centre of pressure (CoP) outcomes during balance measurements for both the non-affected and affected legs across three conditions (Eyes Open, Eyes Closed, Eyes Closed + Dual-Task) for HC, OIP, and SP groups. The table presents CoP path length (cm) and range of motion (ROM) in the anteroposterior (AP) and mediolateral (ML) directions.

Balance: Centre of Pressure Parameters	**Eyes Open**			**Eyes Closed**			**Eyes Closed + Dual-Task**		
Groups	**HC**	**OIP**	**SP**	**HC**	**OIP**	**SP**	**HC**	**OIP**	**SP**
Non-affected leg outcomes									
CoP path length (cm) Mean ± SD	69.9±8.9	63.9±7.2	85.1±15.0	71.1±10.9	111.0±45.9	203.5±102.3	84.5 ±7.3	113.4±31.1	247.7±154.3
AP/ML ROM (cm)	0.61 / 3.28	0.63 / 3.63	1.05 / 5.26	0.45 / 2.23	0.83 / 4.61	1.02 / 7.78	0.60 / 2.94	0.72 / 4.55	1.94 / 8.56
Affected leg outcomes (Mean ± SD)									
CoP path length (cm) Mean ± SD	58.4±9.3	61.9±19.1	44.4±9.6	62.3±13.7	69.6±19.5	51.6 ± 6.6	71.8±17.0	73.1±20.7	60.6±3.0
AP/ML ROM (cm)	0.46 / 2.80	0.50 / 1.48	0.59 / 1.63	0.36 / 2.04	0.79 / 1.53	0.60 / 1.75	0.52 / 2.61	0.74 / 1.78	0.93 / 2.31

For the NA leg, CoP path length was lowest in the Eyes Open condition for all groups, with HC exhibiting the shortest path (69.9 cm), followed by OIP (63.9 cm) and SP (85.1 cm). Path length increased in the Eyes Closed and Eyes Closed + Dual-Task conditions, particularly in the OIP and SP groups, with SP showing a strong increase (247.7 cm in Eyes Closed + Dual-Task).

For the affected leg, CoP path length also increased across conditions, but values were generally more consistent between groups. In the Eyes Open condition, path lengths were similar between HC (58.4 cm), OIP (61.9 cm), and SP (44.4 cm), with SP showing the smallest path length in the Eyes Closed condition (51.6 cm). However, increases were observed in the Eyes Closed and Eyes Closed + Dual-Task conditions for all groups.

In the AP/ML ROM of the NA leg, ROM values in both directions were higher for SP across all conditions, indicating greater instability. For the affected leg, SP exhibited the largest ROM increase, particularly in the ML direction, under more challenging conditions, while these stayed more consistent for the other groups.

3.3.2 Loading distributions

Table 8: Loading distribution outcomes for both the non-affected (NA) and affected (A) legs, and symmetry index values across three conditions (Eyes Open, Eyes Closed, Eyes Closed + Dual-Task) for HC, OIP, and SP groups.

Loading Distribution	**Eyes Open**			**Eyes Closed**			**Eyes Closed with Dual-task**		
Groups:	**HC**	**OIP**	**SP**	**HC**	**OIP**	**SP**	**HC**	**OIP**	**SP**
Load dist. NA/A	49.6/50.4	55.9/44.2	52.1/47.9	49.3/50.7	60.9/39.1	55.8/44.2	49.3/50.7	60.7/39.3	56.5/43.5
Symmetry index (Mean ± SD)	-1.6±4.9	23.2±18.6	8.3±30.6	-2.7±6.2	43.6±28.6	23.2±28.7	-2.9±3.8	42.9±24.9	26.2±27.0

Table 10 shows the CoP outcomes for the NA and affected legs for the balance trials. For the force distribution between legs, the HC group maintained an even distribution across all conditions, as is expressed in the SI-values. In contrast, the OIP and SP groups showed more loading towards the NA leg, especially under more challenging conditions. In the Eyes Closed and Eyes Closed + Dual-Task conditions, the OIP group had a higher load on the NA leg, while the SP group exhibited similar outcomes. Although the force distribution as a percentage shows a relatively small difference between the OIP and SP groups for loading, the SI shows that, especially under the more challenging conditions, the OIP group shows a greater asymmetry in loading of the legs.

4. Discussion

The aim of this study was to explore sensitive biomarkers of the altered gait biomechanics and balance control in people with an OIP versus people with a SP and versus able-bodied individuals, conducted through a quantitative biomechanical analysis.

4.1 Gait

4.1.1 Spatiotemporal parameters

In terms of spatiotemporal measures, the results confirm that OIP users generally exhibit gait patterns more similar to HC, while SP users show more pronounced deviations, particularly in cadence and step length of the affected leg. When comparing both prosthesis groups to HC, a prolonged stance phase was observed in the NA leg and a shortened stance phase in the affected leg, consistent with similar previous studies (69-72). This stance-phase asymmetry reflects compensatory strategies in which amputees rely more on the intact limb for propulsion and balance because the prosthetic leg is either less stable or not fully trusted during weight acceptance. As Gard (2006) described, insufficient knee flexion during early stance (≈10% of the gait cycle) limits smooth weight transfer, creating the need for increased hip motion on the NA side to ensure foot clearance for the prosthetic leg. This prolongs stance time on the NA side and reduces stance time on the affected side. This is also supported by the absence of a clear knee flexion peak at 10% (Figure 13), as it limited shock absorption and comfort, makes users less willing to bear weight on the prosthetic leg.

SP users walked with lower cadence and longer step lengths than HC in IS and SSS, though differences were smaller at SSS. This gait pattern likely reflects a compensatory strategy to improve stability and comfort when using a SP. By taking fewer, longer steps, SP users reduce the number of loading cycles per distance walked, minimizing shear and pressure at the socket-skin interface and allowing more time for controlled weight transfer. Although this strategy increases stability, it also reduces walking efficiency and contributes to slower overall speed. In contrast, OIP users demonstrated spatiotemporal parameters closer to HC, reflecting improved load transfer and comfort provided by the direct skeletal connection of the implant. These findings align with earlier research showing that SP users typically exhibit greater gait asymmetries, while OIP users tend toward more symmetric and efficient walking patterns (42).

Minor discrepancies between implied and reported walking speeds are attributable to step exclusion and rounding, rather than physiological differences. The results of Welke et al. (2023) support these findings, showing step-length asymmetry in SP users, while OIP users achieved more symmetric step lengths (73). Stride times remained equal between legs within each group, as expected in bipedal gait, where both limbs complete one stride within the same duration.

4.1.2 Kinematics and Kinetics

Ankle

Both prosthetic groups demonstrated reduced ankle dorsiflexion peaks and diminished push-off on the affected side, which indicates a reduced contribution of the ankle to propulsion. This reduction in movement is consistent with mechanical limitations of energy-storing prosthesis, as have been used by all prosthetic participants. These prosthetic feet, made from carbon fibre, can store and release energy during gait but, lacking active plantarflexion from the gastrocnemius and soleus, cannot generate comparable power to a biological limb
This reduced function is also seen in the kinetic outcomes, where for both prosthetic groups there is a weaker plantar flexion moment during the stance phase. The energy-storing prosthesis can only push back with the

energy stored in it up till that moment, and unless there is active plantar flexion, will lack the energy to produce a similar force as a natural limb.

For the NA legs, these are similar to HC for both angles and moments, but there are later peaks in late stance for SP, as there is a relatively longer stance phase during gait.
The combination of reduced dorsiflexion range and ankle moment generation underscores the passive nature of energy-storing prosthetic ankle function. Additionally, this highlights the current dependence on more proximal segments to restore propulsion and a gait cycle similar to HC, as is discussed further below.

In able-bodied individuals, the propulsive power which is needed during the step-to-step transition in gait, is mainly provided by the ankle, and to a lesser extent by the hip (74). To avoid compensation in the residual hip or contralateral side, the prosthetic foot must provide enough power (75, 76). This further underlines the need for advancements of the prosthetic feet besides the usage of a MPK in transfemoral amputees.

Knee

In both prosthetic groups, the affected side showed reduced flexion during the loading response, even though all participants used MPKs. Despite the advanced features of MPKs, they did not flex adequately during the loading response phase, which is essential for shock absorption and stabilization. The absence of this motion demonstrates that MPKs do not replicate the natural knee response during loading, leading to insufficient shock absorption and higher strain on other joints.

The kinetic results further reinforce this observation. For the affected leg, both OIP and SP groups displayed reduced or absent extension moment peaks during the loading response, and terminal swing compared to HC. As stated before, this shows a limited ability of the MPK to stabilize during the weight acceptance.

The NA legs of the prosthetic groups showed knee flexion patterns comparable to HC. However, the kinetic outcomes indicate altered loading dynamics in the NA-leg influenced by the affected limb, as reflected by the absence of a clear early stance extension peak, and an altered flexion peak at terminal stance for the SP group. This may represent a compensatory mechanism, in which the NA leg adapts its movement pattern to mimic the affected limb in an attempt to increase gait symmetry.
For the knee adduction moment in the NA-leg, interpretation is limited due to the large inter-participant variability in both prosthetic groups. On the affected side, both groups followed the HC pattern but with lower peaks, particularly at initial stance and the terminal stance). When comparing OIP and SP, the OIP follows the HC group more closely with the abduction peaks. These lower peaks suggest decreased loading, which reflects the unloading strategy to minimize pressure and instability on the prosthetic limb. The closer resemblance of OIP to the HC pattern suggests that the direct skeletal connection allows more natural load transfer compared to SP. Together, these results illustrate that limited knee motion and altered load transfer in both prosthetic groups place greater mechanical demands on the hip, contributing to proximal compensations observed in gait. This reduced dynamic response not only limits shock absorption but also increases metabolic cost and reduces overall gait efficiency. However, OIP users appear to show partial improvement in efficiency, as Kooiman et al. (2023) reported intermediate oxygen consumption values between SP users and HC (77).

Hip

In contrast to the knee, hip kinematics were largely preserved in flexion/extension across groups.
On the affected side, SP users demonstrated constant hip abduction over the entire gait cycle while OIP users showed adduction in stance, which indicates differing stabilization strategies. However, considerable inter-participant variability was observed, particularly during the swing phase in SP users. Both groups deviated from the HC pattern, with greater abduction seen in SP. Both groups deviated from the HC pattern, with the greater abduction seen in SP users likely reflecting a compensatory strategy to increase stability through a wider BoS.

For hip rotation, the affected limbs of both prosthetic groups roughly followed the HC pattern, although large within-group variability was present. On the NA-side, OIP users more closely resembled the HC group than SP users, indicating improved rotational control and alignment symmetry, likely due to the more direct skeletal connection provided by osseointegration.

Kinetically, the graphs reveal that hip moments of the prosthesis groups at heel strike on the NA side followed a similar trend to HC, showing that the NA side for all groups still generates propulsive forces. But for the affected side the initial peaks are lower or absent in both prosthetic groups. For the flexion and adduction moments, the OIP users produce patterns more similar to the HC when compared to SP. This shows that OIP promotes more natural gait, even though it still needs to compensate for lacking a natural knee and ankle.
For the hip rotation moments, both prosthetic groups showed reduced external rotation peaks compared to HC, showing limited rotational control of the prosthetic limb during stance.
These interpretations align with findings by Ekdahl et al. (2025), who reported greater hip abductor force production in OIP users, suggesting potential long-term adaptation of hip musculature following osseointegration (39). However, in the short term, these users may still experience reduced mechanical leverage and altered muscle coordination, particularly when residual limb length has been limited.

Trunk Lean

Trunk leaning is a commonly observed compensatory strategy to reduce hip abductor demand, particularly in individuals with muscle weakness or those walking with lower-limb prostheses. In these cases, individuals lean their trunk toward the weakened side to reduce the demand on the hip abductors and maintain stability (7, 8). As seen in Figure 13 for the curve of the trunk lean, for both prosthesis groups, there is lateral trunk lean towards the affected side. This shows that both prosthesis groups lack to generate the required hip abduction moment (Glut. medius, Glut, minimus, and Tensor Fasciae Latae function) to stabilize the pelvis with their abductors alone during single support. This is especially the case for the OIP group, as during the entire measurement, the gait cycle for this group has a trunk lean towards the affected leg.

In TFAs, compensatory trunk leaning can lead to back pain, which has been reported in TFAs (78, 79). Therefore, the goal is to prevent this compensatory behaviour in patients to prevent or alleviate pain, but also to regain a more natural gait and to minimize discomfort. The results found in this study demonstrate an opposite trend compared to previous research concerning the trunk lean, with OIP user showing greater trunk lean than SP users. In summary, the pronounced trunk lean, especially in OIP users, suggests that improved mechanical attachment alone does not restore full frontal-plane stability or eliminate compensatory upper-body movements.

Overall

One explanation for the compensatory mechanisms, is that OIP users are often described as having shorter or problematic residual limbs, although there is little evidence which compares length directly between OIP and SP users (80, 81) . A shorter femur means a shorter lever arm, which reduces hip abductor efficiency, increasing the need for a compensatory trunk lean to maintain pelvic stability during stance. Research by Geertzen et al (2019), states that a longer residual limb is more beneficial for gait parameters and providing lever arm (82). For TFAs in general, it was found that isometric hip moments and hip abduction strength was only ~60% of that in able-bodied individuals (83). But also In a study conducted by Gailey et al. (2023), comparing OIP and SP, residual limb length was reported to have a moderate influence on gait velocity, as OIP users, with a shorter residual limb length, walked slower the SP users (84).

Secondly, OI improves direct load transfer and comfort but is does not directly restore muscle strength and coordination. Amputation leads to muscle atrophy, especially shorter residual limbs (85), and creating a stump after amputation also alters the line of action of the muscle (86). These structural and functional differences may limit the capacity of the hip abductors to stabilize the pelvis effectively, thereby contributing to increased

trunk lean despite the improved mechanical connection provided by osseointegration, which can explain the results found in this research.
All these kinematic findings align with previous research in SP users, which shows that even with MPKs, TFAs often show reduced knee flexion during loading, leading to compensatory strategies at the hip and ankle (87). This highlights the complexity of replicating natural gait mechanics in prosthetic design and highlights the continued need for advancements in knee control and overall prosthetic function for SP as well as OIP.

Both OIP and SP users show reduced hip extension at terminal swing in the affected side, meaning the residual limb can not decelerate the forward swinging leg effectively. This shows that prosthesis users have less control of controlling limb placement for heel strike. This affects the transition into stance, which leads to less effective weight acceptance and reducing propulsion efficiency later in the gait cycle.

4.1.3 Margin of Stability

In terms of dynamic stability, our study revealed differences in the MoS between prosthesis groups. Both OIP and SP groups had similar AP MoS values, indicating comparable forward stability, but differences were observed in the ML direction. SP users exhibited a negative mean MoS on the NA side and affected side, suggesting reduced lateral stability compared to OIP users, who maintained a slightly positive MoS. This indicates that, despite both groups experiencing challenges with ML stability when compared to HC, OIP users show a more stable balance profile overall. It should be noted that these ML MoS values were small in magnitude and close to zero and accompanied by large variability. Therefore, while the negative mean values may indicate reduced lateral stability, these findings should be seen as indicative of a trend rather than a definitive difference.

The BoS used in this research, was approximated using the SMH and HEE markers (most anterior and most proximal markers on the foot). However, a recent study by Millard and Sloot (2025), showed that a functional BoS (fBoS) provides more accurate and functional representations of the BoS, than the marker based BoS approximations (88). The fBoS accounts for the weight-bearing area, instead of all the area which touches the ground. They found that the fBoS is around 23% smaller in area, showing that the traditional BoS may overestimate the stabilizing support of the foot (88). Millard and Sloot performed the research for static trials, not within gait trials, leading to the possibility that the differences between fBoS and marker-based BoS might be different during dynamic gait conditions, especially when also taking into account that amputees have altered weight-bearing and prosthetic feet (88). Exploring the fBoS during gait could therefore be valuable for future research, as it may improve the accuracy of MoS in gait calculations and better capture stability in clinical populations.

4.2 Balance

Based on the CoP outcomes in Table 9 , SP users show significantly larger increases in CoP path length and ML range when visual input was removed, indicating a greater reliance on visual feedback for balance control. OIP users, while still affected by Dual-Tasking, exhibited less sway, suggesting that the OIP may offer more stability for both legs during sensory challenges. It should be noted that, for the affected leg, the SP group shows a lower CoP length in all balance trials when compared to both OIP and HC. This should be seen in combination with the CoP length of the NA-leg, where a large compensation in CoP is needed to maintain a stable stance.
When looking into the loading distributions, we see that the SP group has a more evenly distributed loading than the OIP, which is further confirmed by a lower SI value. As described in Table 4 (Classification of Symmetry Index), the outcome Table 10 shows that both OIP and SP groups exhibit high asymmetry in all trials, except for the Eyes Open trial for SP, where the SI is low but accompanied by a relatively large variability.
These outcomes suggest that balance in SP patients is not necessarily more unevenly distributed than in OIP patients, but it is less consistently controlled between the legs.

4.3 Limitations

4.3.1 Participants and prosthesis characteristics

The study included a relatively small sample (HC: n = 5, OIP: n = 5, SP: n = 3), which makes the results biased from variability between participants. A larger cohort would improve the generalizability and reliability of the findings, including a statistical analysis. Stump length was not included in the analysis, even though it can influence gait efficiency by affecting muscle function in both prosthetic groups. In addition, the duration of OIP use was not recorded, which may have influenced outcomes, as individuals with less experience may not have fully adapted to this type of prosthesis compared to long term SP users.

4.3.2 Treadmill versus overground walking

All measurements were performed on a treadmill, a setting to which not all participants were familiar. Treadmill walking differs from overground walking in that the body remains stationary while the legs move beneath it, which may influence step length, cadence, and perceived stability, particularly at lower speeds. An alternative approach performing measurements over force plates in a runway setting. However, this leads to another problem, where participants need to turn around after a fixed distance. Although treadmill walking allows for continuous movement and measurement without interruptions or turning, it still may not fully represent natural overground gait patterns participants exhibit in daily life.

4.3.3 Walking speed

Trials for IS and SSS were measured and analysed, but speed normalization based on leg length or body size was not added within this study. Since preferred walking speed varied among participants, some exceeded 1 m/s, while others walked slower, potentially introducing variability in parameters. Controlling a normalized gait speed instead of an IS could have reduced differences between participants and allowed more direct comparisons between groups.

4.3.4 Balance assessment

In this study, balance assessment was restricted to CoP data from static trials, with no separate evaluation of dynamic balance. Future protocols could include dynamic stance trials, in which participants are instructed to shift their CoP in controlled, slow circular movements without foot displacement, similar to procedures described in Millard and Sloot (2025) (88).

4.3.5 Symmetry Index

The SI was used to quantify loading between legs, but this metric does not capture the timing of weight shifts during stance, taking a mean over the entire 20-second trials. As a result, SI values may oversimplify balance control, particularly when participants alternate dominance between legs within a trial.

4.3.6 Technical considerations.

Marker placement on shoes, clothing, or in individuals with higher body fat and soft tissue may have affected marker accuracy due to relative motion between the marker and the targeted anatomical landmark, potentially introducing error.

Another consideration for interpretation of the results should be that the accuracy of joint angle estimations in OpenSim is typically within 3–4°, with errors largely driven by marker placement (42). A study by Dunne et al. (2021), suggests that manual placement introduces around 3.7° Root Mean Square (RMS) error, whereas optimized registration can reduce this to ~1.2°. Such errors work through into joint moment calculations. Finally, the metatarsophalangeal (MTP) and subtalar joints were locked in the musculoskeletal models to simplify analysis, particularly for the prosthesis legs where these joints are completely absent. To be consistent for comparisons between and within groups and simplification, for the NA, these joints were locked. However, this may have affected ankle kinematics and kinetics, limiting the physiological accuracy of the results.

5. Conclusion

5.1 Clinical Implications

This study sheds light on the similarities and differences between OIP and SP in terms of gait-biomechanics and balance performance, and the possible gain in switching from SP to OIP. Both OIP and SP users differ from HC, as they both show reduced knee flexion during loading and impaired lateral stability, requiring compensations at the hip and trunk. Spatiotemporally, OIP users generally approached healthy patterns more closely than SP users and demonstrated a more favourable ML MoS. Clinically, these findings suggest that OIP promotes a more symmetrical gait, with cadence, step length, and stability parameters approaching those of HC. In contrast, SP users displayed longer step lengths, lower cadence, and increased reliance on the NA limb. Rehabilitation for both groups should target hip abductor strength, trunk control, and restoration of loading-response knee flexion to reduce compensatory movements and resulting discomfort. For SP users in particular, interventions focusing on dynamic balance training and lateral stability may be beneficial. During the balance trials, SP users relied more on visual input and showed less consistent leg-to-leg control, suggesting rehabilitation should target balance and weight distribution training. OIP users show improved stability under sensory challenges, but therapy should focus on trunk control to maximize functional benefits.
In summary, these findings indicate that OIP promotes a gait pattern closer to that of HC when compared to SP users. OIP users show more symmetrical and stable balance, whereas the SP users demonstrate greater compensatory strategies, reliance on the non-affected limb. And increased sway under sensory-challenging conditions.

5.2 Future Directions

Future research should aim to examine the long-term clinical impact of these observed differences between OIP and SP use. Large-scale, longitudinal studies could clarify whether the more normalized loading and stability seen in OIP users also translates into lower risks of secondary musculoskeletal conditions, such as hip or knee osteoarthritis, compared to SP users.

Additionally, research is needed, such as on propulsive force through GRF data or OpenSim simulations, to look into internal joint power during gait. This helps to explore whether targeted training and prosthetic adjustments can prevent the specific gait deviations seen in OIP and SP users, such as reduced knee flexion in loading and trunk leaning. Integrating muscle activity measurements, such as Electromyography (EMG), and energy expenditure measurements can further provide insight into the efficiency of the stump muscles when walking with a prosthesis and using compensatory strategies. Finally, comparing biomechanical outcomes with patient-reported outcomes measures for comfort, mobility, and quality of life are crucial to determine the broader clinical value of OIP compared to SP and guide personalised rehabilitation strategies.

6. Disclosure Generative AI

Within this research project, generative AI tools were used to support both data processing and writing. The primary tools applied were ChatGPT (OpenAI) and Google Gemini (Google).

ChatGPT was used to adjust existing Python scripts, which were written by supervisors, and to generate new scripts for processing measurement data and automate the OpenSim tasks. To safeguard data privacy, no real patient data were used as input. To provide examples to the AI, dummy files with a similar structure were created. All AI-generated scripts and their outputs were verified for correctness and adjusted if necessary. ChatGPT was also used to improve code readability by generating comments for text blocks.

Google Gemini was used during the thesis writing phase for grammar checking, identifying redundant explanations, and suggesting clearer sentence structures. AI suggestions were only incorporated when they improved clarity and readability without altering the intended meaning.

All AI-generated outputs were critically evaluated prior to implementation. The use of these tools primarily aimed to improve efficiency, consistency, and readability. Their use was comparable to discussing subjects with a fellow student or supervisor for coding support or a writing partner for feedback, while final responsibility for all content remained with the author.

7. Acknowledgements

After seven years of studying, I am grateful to finally hand in this Master Thesis. I am thankful for all the opportunities I have received throughout these years, which have helped me grow both academically and personally. Over the past year, there have been many times when I felt pessimistic and overwhelmed about this project. I am deeply grateful to those around me who patiently listened to my complaints about patient scheduling, Python programming, medical ethics approval, modelling, and reimbursements.

To my supervisors, this project could not have succeeded without the guidance of **Mariska**, who was always quick to respond to my emails and helped me set up the project. I would also like to thank **Jaap**, who took over supervision from Mariska and contributed his experience and expertise during the final stages of my thesis. I want to thank **Oscar** for his help in finding and selecting suitable participants, allowing me to join him in the operating room, and showing me that not everything I wrote or explained was as clear as it seemed to me.

My thanks go to all participants for taking the time to come to Erasmus MC for measurements and for sharing your experiences of living with an amputation, or just for the sake of helping me measure an able-bodied.

I also thank the **MOBI-lab supervisors** for assisting me with setting up and processing the measurements, and for their valuable feedback during the Clinical Biomechanics Meetings. I still owe you a clipstick workshop as the current MOBI clipstick resident!

A big thank you to the secretaries, **Nancy, Annet, and Simone**, for helping plan meetings, reserve rooms, and contacting physicians.

And of course, to **Sarah**, thank you for helping me through countless stressful moments, for thinking along when I was stuck with a negative thought, and for helping me take my mind off the thesis when needed.

I am endlessly grateful to **my parents** for every opportunity they have given me to pursue my dreams. I know you always believed in me, from the time I forgot to prepare my elementary school speech on American football, where my father helped me write reports, to the moments I withheld my poor French exam results, and even during the early bachelor years when I questioned whether I was suited to study Technical Medicine. Thank you for making it all possible.

And finally, I want to thank **God**, He always knows what’s in the depth’s of my heart. He knows me inside and out. I am thankful for the Talents he has given me, and the people around me to bring them to flourish. I am excited for what the future holds, hoping I can continue to develop myself, and help both the familiar and new people along the way!

Alexander Hendrik Kuipers
Habakuk 3: 17-19
Rotterdam, October 2025

8. Bibliography

1. Revalidatie Z. Beenamputatie Poliklinische Revalidatie Dagbehandeling. In: Revalidatie Z, editor. 2017.
2. Nederland telt bijna 1,2 miljoen mensen met diabetes 2024 [Available from: https://www.nivel.nl/nl/nieuws/nederland-telt-bijna-12-miljoen-mensen-met-diabetes#:~:text=In%202022%20waren%20er%20in,te%20weinig%20insuline%20aangemaakt%20worden.
3. Penn-Barwell JG. Outcomes in lower limb amputation following trauma: a systematic review and meta-analysis. Injury. 2011;42(12):1474-9.
4. Raya MA, Gailey RS, Fiebert IM, Roach KE. Impairment variables predicting activity limitation in individuals with lower limb amputation. Prosthet Orthot Int. 2010;34(1):73-84.
5. Peters EJ, Childs MR, Wunderlich RP, Harkless LB, Armstrong DG, Lavery LA. Functional status of persons with diabetes-related lower-extremity amputations. Diabetes Care. 2001;24(10):1799-804.
6. Prosthetics through the ages NIH MedlinePlus 2023.
7. Thurston AJ. Pare and prosthetics: the early history of artificial limbs. ANZ J Surg. 2007;77(12):1114-9.
8. Blatchford. SmartIP microprocessor controlled knee [Available from: https://www.blatchfordmobility.com/en-us/products/knees/smartip.
9. Prothesensystem C-Leg schreibt einzigartige Erfolgsstory 2011 [Available from: https://www.management-krankenhaus.de/topstories/medizintechnik/prothesensystem-c-leg-schreibt-einzigartige-erfolgsstory.
10. Martin J, Pollock A, Hettinger J. Microprocessor Lower Limb Prosthetics: Review of Current State of the Art %U https://journals.lww.com/jpojournal/fulltext/2010/07000/microprocessor_lower_limb_prosthetics__review_of.10.aspx. JPO: Journal of Prosthetics and Orthotics. 2010;22(3):183-93.
11. Henao SC, Orozco C, Ramirez J. Influence of Gait Cycle Loads on Stress Distribution at The Residual Limb/Socket Interface of Transfemoral Amputees: A Finite Element Analysis. Sci Rep. 2020;10(1):4985.
12. Hagberg K, Branemark R. Consequences of non-vascular trans-femoral amputation: a survey of quality of life, prosthetic use and problems. Prosthet Orthot Int. 2001;25(3):186-94.
13. Lyon CC, Kulkarni J, Zimerson E, Van Ross E, Beck MH. Skin disorders in amputees. J Am Acad Dermatol. 2000;42(3):501-7.
14. Frolke JP, van de Meent H. [The endo-exo prosthesis for patients with a problematic amputation stump]. Ned Tijdschr Geneeskd. 2010;154:A2010.
15. Butler K, Bowen C, Hughes AM, Torah R, Ayala I, Tudor J, et al. A systematic review of the key factors affecting tissue viability and rehabilitation outcomes of the residual limb in lower extremity traumatic amputees. J Tissue Viability. 2014;23(3):81-93.
16. Hagberg K, Brånemark R. One hundred patients treated with osseointegrated transfemoral amputation prostheses-Rehabilitation perspective. J Rehabil Res Dev. 2009;46(3):331-44.
17. Hagberg K, Häggström E, Uden M, Brånemark R. Socket versus bone-anchored trans-femoral prostheses:: Hip range of motion and sitting comfort. Prosthetics and Orthotics International. 2005;29(2):153-63.
18. Agarwal S, Mistry L, Mistry S, Kadam I, Bhiwapurkar S, Talekar S, et al. The Per-Ingvar Branemark Era (1929-2014): Evolution of a No Compromise Prosthetic Dental Replacement. Cureus. 2024;16(10):e71708.
19. Marin E, Lanzutti A. Biomedical Applications of Titanium Alloys: A Comprehensive Review. Materials (Basel). 2023;17(1).
20. Branemark PI, Bo H, Adell R, Breine U, Lindström J, Hallén O, et al. Osseointegrated implants in the treatment of the edentulous jaw. Experience from a 10-year period. Scandinavian journal of plastic and reconstructive surgery Supplementum. 1977;16:1-132.
21. Branemark PI. Osseointegration and its experimental background. J Prosthet Dent. 1983;50(3):399-410.
22. Li Y, Branemark R. Osseointegrated prostheses for rehabilitation following amputation : The pioneering Swedish model. Unfallchirurg. 2017;120(4):285-92.
23. Brånemark R. A biomechanical study of osseointegration. In-vivo measurements in rat, rabbit, dog and man1996.
24. Banducci E, Al Muderis M, Lu W, Bested SR. The safety of one-stage versus two-stage approach to osseointegrated prosthesis for limb amputation. Bone Jt Open. 2023;4(7):539-50.

25. Hagberg K, Ghassemi Jahani SA, Kulbacka-Ortiz K, Thomsen P, Malchau H, Reinholdt C. A 15-year follow-up of transfemoral amputees with bone-anchored transcutaneous prostheses. Bone Joint J. 2020;102-B(1):55-63.
26. Understanding Osseointegration Surgery [Available from: https://osseointegration.org/osseointegration/.
27. Gaffney BMM, Davis-Wilson HC, Christiansen CL, Awad ME, Lev G, Tracy J, et al. Osseointegrated prostheses improve balance and balance confidence in individuals with unilateral transfemoral limb loss. Gait Posture. 2023;100:132-8.
28. Hagberg K, Häggström E, Jönsson S, Rydevik B, Brånemark R. Psychoprosthetics. Chapter: Osseoperception and osseointegrated prosthetic limbs2008.
29. Toderita D, McGuire T, Benton AM, Handford C, Ramasamy A, Hindle P, et al. A one-year follow-up case series on gait analysis and patient-reported outcomes for persons with unilateral and bilateral transfemoral amputations undergoing direct skeletal fixation. J Neuroeng Rehabil. 2024;21(1):208.
30. Leijendekkers RA, van Hinte G, Nijhuis-van der Sanden MW, Staal JB. Gait rehabilitation for a patient with an osseointegrated prosthesis following transfemoral amputation. Physiother Theory Pract. 2017;33(2):147-61.
31. Bhatnagar VM, Karani JT, Khanna A, Badwaik P, Pai A. Osseoperception: An Implant Mediated Sensory Motor Control- A Review. J Clin Diagn Res. 2015;9(9):Ze18-Ze20.
32. Van de Meent H, Hopman MT, Frolke JP. Walking ability and quality of life in subjects with transfemoral amputation: a comparison of osseointegration with socket prostheses. Arch Phys Med Rehabil. 2013;94(11):2174-8.
33. Muderis MA, Lu W, Glatt V, Tetsworth K. Two-Stage Osseointegrated Reconstruction of Post-traumatic Unilateral Transfemoral Amputees. Mil Med. 2018;183(suppl_1):496-502.
34. Leijendekkers RA, van Hinte G, Frolke JP, van de Meent H, Atsma F, Nijhuis-van der Sanden MW, et al. Functional performance and safety of bone-anchored prostheses in persons with a transfemoral or transtibial amputation: a prospective one-year follow-up cohort study. Clin Rehabil. 2019;33(3):450-64.
35. Ontario H. Osseointegrated Prosthetic Implants for People With Lower-Limb Amputation: A Health Technology Assessment. Ont Health Technol Assess Ser. 2019;19(7):1-126.
36. Hoellwarth JS, Al-Jawazneh S, Oomatia A, Tetsworth K, Al Muderis M. Transfemoral Osseointegration for Amputees with Well-Managed Diabetes Mellitus. JB JS Open Access. 2024;9(4).
37. Gailey R, Allen K, Castles J, Kucharik J, Roeder M. Review of secondary physical conditions associated with lower-limb amputation and long-term prosthesis use. J Rehabil Res Dev. 2008;45(1):15-29.
38. Golyski PR, Potter BK, Forsberg JA, Hendershot BD. Comparing the mechanical energetics of walking among individuals with unilateral transfemoral limb loss using socket and osseointegrated prosthetic interfaces. Sci Rep. 2025;15(1):9755.
39. Ekdahl MA, Vandenberg NW, Melton DH, Hendershot BD, Christiansen CL, Stoneback JW, et al. Transfemoral bone-anchored limb use changes dynamic hip muscle forces during walking. J Biomech. 2025;183:112620.
40. Thomsen PB, Gaffney BMM, Tracy JB, Vandenberg NW, Awad ME, Christiansen CL, et al. Cumulative loading increases and loading asymmetries persist during walking for people with a transfemoral bone-anchored limb. Gait Posture. 2024;113:46-52.
41. Vandenberg NW, Stoneback JW, Davis-Wilson H, Christiansen CL, Awad ME, Melton DH, et al. Unilateral transfemoral osseointegrated prostheses improve joint loading during walking. J Biomech. 2023;155:111658.
42. Ranaldi S, Naaim A, Marchis C, Robert T, Dumas R, Conforto S, et al. Walking ability of individuals fitted with transfemoral bone-anchored prostheses: A comparative study of gait parameters. Clin Rehabil. 2023;37(12):1670-83.
43. Gait Cycle Coachhackfeet [Available from: https://www.coachhackfeet.com/blog/2026277_gait-cycle.
44. Jayakaran P, Johnson GM, Sullivan SJ. Postural control in response to altered sensory conditions in persons with dysvascular and traumatic transtibial amputation. Arch Phys Med Rehabil. 2015;96(2):331-9.
45. Lusardi MM, Bowers DM. Motor control, motor learning, and neural plasticity in orthotic and prosthetic rehabilitation. Orthotics & prosthetics in rehabilitation. 2013:38-53.
46. Geurts AC, Mulder TW, Nienhuis B, Rijken RA. Postural reorganization following lower limb amputation. Possible motor and sensory determinants of recovery. Scand J Rehabil Med. 1992;24(2):83-90.
47. Rougier PR, Bergeau J. Biomechanical analysis of postural control of persons with transtibial or transfemoral amputation. Am J Phys Med Rehabil. 2009;88(11):896-903.
48. Meyer C, Killeen T, Awai CE, Curt A, Bolliger M, Linnebank M, et al. Familiarization with treadmill walking: How much is enough? Scientific Reports. 2019;9.

49. Leboeuf F, Baker R, Barre A, Reay J, Jones R, Sangeux M. The conventional gait model, an open-source implementation that reproduces the past but prepares for the future. Gait Posture. 2019;69:235-41.
50. Laboeuf F. CGM 2.5 - [Available from: https://pycgm2.netlify.app/cgm/cgm2.5/.
51. M-Gait: The High-Tech Modular Treadmill System [Available from: https://www.motekmedical.com/solution/m-gait/.
52. D-Flow: Your Total Integration Platform [Available from: https://www.motekmedical.com/software/d-flow/.
53. Vicon [Available from: https://www.vicon.com/.
54. Vicon Nexus [Available from: https://www.vicon.com/software/nexus/.
55. H/P/Cosmos: Chestbelt system XL safety arch harness [Available from: https://www.hpcosmos.com/en/products/supplies-options/chestbelt-system-xl-safety-arch-harness.
56. Delp SL, Anderson FC, Arnold AS, Loan P, Habib A, John CT, et al. OpenSim: open-source software to create and analyze dynamic simulations of movement. IEEE Trans Biomed Eng. 2007;54(11):1940-50.
57. Hicks J. Gait 2392 and 2354 Models Opensim Documentation2024 [Available from: https://opensimconfluence.atlassian.net/wiki/spaces/OpenSim/pages/53086215/Gait+2392+and+2354+Models.
58. Raveendranathan V, Carloni R. Musculoskeletal Model of an Osseointegrated Transfemoral Amputee in OpenSim. 2020 8th IEEE RAS/EMBS International Conference for Biomedical Robotics and Biomechatronics (BioRob). 2020:1196-201.
59. LaPre AK, Price MA, Wedge RD, Umberger BR, Sup FCt. Approach for gait analysis in persons with limb loss including residuum and prosthesis socket dynamics. Int J Numer Method Biomed Eng. 2018;34(4):e2936.
60. Community BO. Blender 3.2.2. 3.2.2 ed. Amsterdam, The Netherlands: Blender Foundation; 2022.
61. Tokuda K, Anan M, Takahashi M, Sawada T, Tanimoto K, Kito N, et al. Biomechanical mechanism of lateral trunk lean gait for knee osteoarthritis patients. J Biomech. 2018;66:10-7.
62. Mikami K, Shiraishi M, Kamo T. Effect of subjective vertical perception on lateral flexion posture of patients with Parkinson's disease. Sci Rep. 2022;12(1):1532.
63. Ma Y, Mithraratne K, Wilson N, Zhang Y, Wang X. Kinect V2-Based Gait Analysis for Children with Cerebral Palsy: Validity and Reliability of Spatial Margin of Stability and Spatiotemporal Variables. Sensors (Basel). 2021;21(6).
64. Hof AL, Gazendam MG, Sinke WE. The condition for dynamic stability. J Biomech. 2005;38(1):1-8.
65. Dussault-Picard C, Tisserand R, Robidou C, Cherni Y. Comparison of marker-based and center-of-pressure-based approaches for calculating the margin of stability. Front Sports Act Living. 2025;7:1571994.
66. Yamaguchi T, Masani K. Effects of age on dynamic balance measures and their correlation during walking across the adult lifespan. Sci Rep. 2022;12(1):14301.
67. Blazkiewicz M, Wiszomirska I, Wit A. Comparison of four methods of calculating the symmetry of spatial-temporal parameters of gait. Acta Bioeng Biomech. 2014;16(1):29-35.
68. Robinson RO, Herzog W, Nigg BM. Use of force platform variables to quantify the effects of chiropractic manipulation on gait symmetry. J Manipulative Physiol Ther. 1987;10(4):172-6.
69. Harandi VJ, Ackland DC, Haddara R, Lizama LEC, Graf M, Galea MP, et al. Gait compensatory mechanisms in unilateral transfemoral amputees. Med Eng Phys. 2020;77:95-106.
70. Gard SA. Use of quantitative gait analysis for the evaluation of prosthetic walking performance. Proceedings of the American Academy of Orthotists and Prosthetists. 2006:P93-P104.
71. Hof AL, van Bockel RM, Schoppen T, Postema K. Control of lateral balance in walking. Experimental findings in normal subjects and above-knee amputees. Gait Posture. 2007;25(2):250-8.
72. Nolan L, Wit A, Dudzinski K, Lees A, Lake M, Wychowanski M. Adjustments in gait symmetry with walking speed in trans-femoral and trans-tibial amputees. Gait Posture. 2003;17(2):142-51.
73. Welke B, Hurschler C, Schwarze M, Jakubowitz E, Aschoff HH, Orgel M. Comparison of conventional socket attachment and bone-anchored prosthesis for persons living with transfemoral amputation - mobility and quality of life. Clin Biomech (Bristol). 2023;105:105954.
74. Zelik KE, Adamczyk PG. A unified perspective on ankle push-off in human walking. J Exp Biol. 2016;219(Pt 23):3676-83.
75. Probsting E, Altenburg B, Bellmann M, Krug K, Schmalz T. How does ankle power on the prosthetic side influence loading parameters on the sound side during level walking of persons with transfemoral amputation? Prosthet Orthot Int. 2022;46(4):306-13.
76. Bonnet X, Villa C, Loiret I, Lavaste F, Pillet H. Distribution of joint work during walking on slopes among persons with transfemoral amputation. J Biomech. 2021;129:110843.

77. Kooiman V, Haket L, Verdonschot N, Leijendekkers R, Weerdesteyn V. Oxygen consumption and gait dynamics in transfemoral bone-anchored prosthesis users compared to socket-prosthesis users: A cross-sectional study. Gait Posture. 2023;103:12-8.
78. Hendershot BD, Wolf EJ. Three-dimensional joint reaction forces and moments at the low back during over-ground walking in persons with unilateral lower-extremity amputation. Clin Biomech (Bristol). 2014;29(3):235-42.
79. Morgenroth DC, Orendurff MS, Shakir A, Segal A, Shofer J, Czerniecki JM. The relationship between lumbar spine kinematics during gait and low-back pain in transfemoral amputees. Am J Phys Med Rehabil. 2010;89(8):635-43.
80. Frolke JP, Atallah R, Leijendekkers R. Press-Fit Bone-Anchored Prosthesis for Patients with Short Transfemoral Amputation. JBJS Essent Surg Tech. 2025;15(1).
81. Hoellwarth JS, Geffner AD, Reif TJ, Rozbruch SR. Transcutaneous Osseointegration for Amputees with Short Residual Bone: Is There Increased Risk for Complications? – A Pilot Study %U https://journals.lww.com/jllr/fulltext/2022/08020/transcutaneous_osseointegration_for_amputees_with.5.aspx. Journal of Limb Lengthening & Reconstruction. 2022;8(2):115-20.
82. Geertzen JHB, de Beus MC, Jutte PC, Otten E, Dekker R. What is the optimal femur length in a trans-femoral amputation? A mixed method study: Scoping review, expert opinions and biomechanical analysis. Med Hypotheses. 2019;129:109238.
83. Heitzmann DWW, Leboucher J, Block J, Gunther M, Putz C, Gotze M, et al. The influence of hip muscle strength on gait in individuals with a unilateral transfemoral amputation. PLoS One. 2020;15(9):e0238093.
84. Gailey RS, Kristal A, Al Muderis M, Lucarevic J, Clemens S, Applegate EB, et al. Comparison of prosthetic mobility and balance in transfemoral amputees with bone-anchored prosthesis vs. socket prosthesis. Prosthet Orthot Int. 2023;47(2):130-6.
85. Leijendekkers RA, Marra MA, Ploegmakers MJM, Van Hinte G, Frolke JP, Van De Meent H, et al. Magnetic-resonance-imaging-based three-dimensional muscle reconstruction of hip abductor muscle volume in a person with a transfemoral bone-anchored prosthesis: A feasibility study. Physiother Theory Pract. 2019;35(5):495-504.
86. Jaegers SM, Arendzen JH, de Jongh HJ. Changes in hip muscles after above-knee amputation. Clin Orthop Relat Res. 1995(319):276-84.
87. Rasheed F, Martin S, Tse KM. Design, Kinematics and Gait Analysis, of Prosthetic Knee Joints: A Systematic Review. Bioengineering (Basel). 2023;10(7).
88. Millard M, Sloot LH. A polygon model of the functional base-of-support during standing improves the accuracy of balance analysis. J Biomech. 2025;192:112927.

9. Supplementary Materials

Appendix A1. Custom Python Scripts

utils.py:

- Contains shared helper functions used across multiple scripts.

Main.py:

- Coordinates the full workflow for all subjects, importing the necessary functions and looping through all files, such running IK and ID processing.

patient_metadata.py:

- Loads dynamic patient metadata from an Excel file and retrieves subject-specific attributes (e.g., affected leg, height, group).

ImportMOBILabDataAHK.py:

- converts .c3d files into .trc and .mot formats, skipping static trials, as these are only need for scaling, which is done manually.

setupfileOS.py:

- Automates generation of .xml setup files for IK and ID analyses in OpenSim. The manually scaled .osim-models are required.

Processing_Gait.py

- Processes .sto files to extract gait phases and compute ensemble averages of kinematic/kinetic data across subjects and groups.

Processing_IKandID.py:

- Aligns IK and ID data based on detected gait cycles and computes group-level ensemble means for comparison.

Processing_Spatiotemporal.py:

- Calculates spatiotemporal gait metrics (e.g., cadence, step length, stance/swing duration) from converted motion data.

Processing_Balance.py:

- Computes CoP-based balance metrics (e.g., sway path, sway area, speed) for each trial and compiles group summaries.

Processing_SPM.py:

- Automates SPM-based comparisons of joint angles and moments between and within groups, saving results as plots and summary tables.

Appendix A2. Pipeline Python scripts

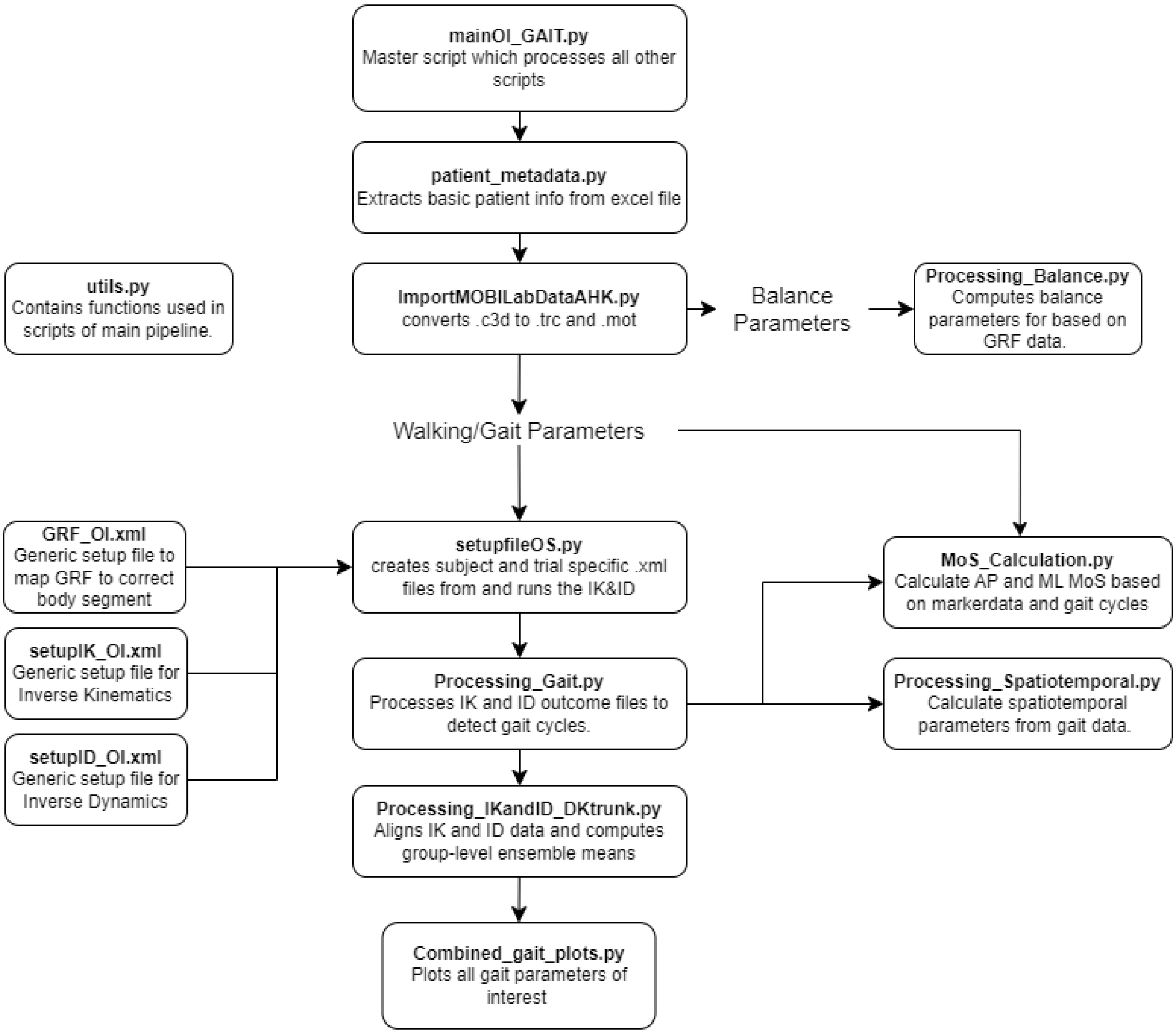

Figure 16: Pipeline of the Python scripts used to process collected data.

Appendix B1. Kinematics Hip joint (1 m/s)

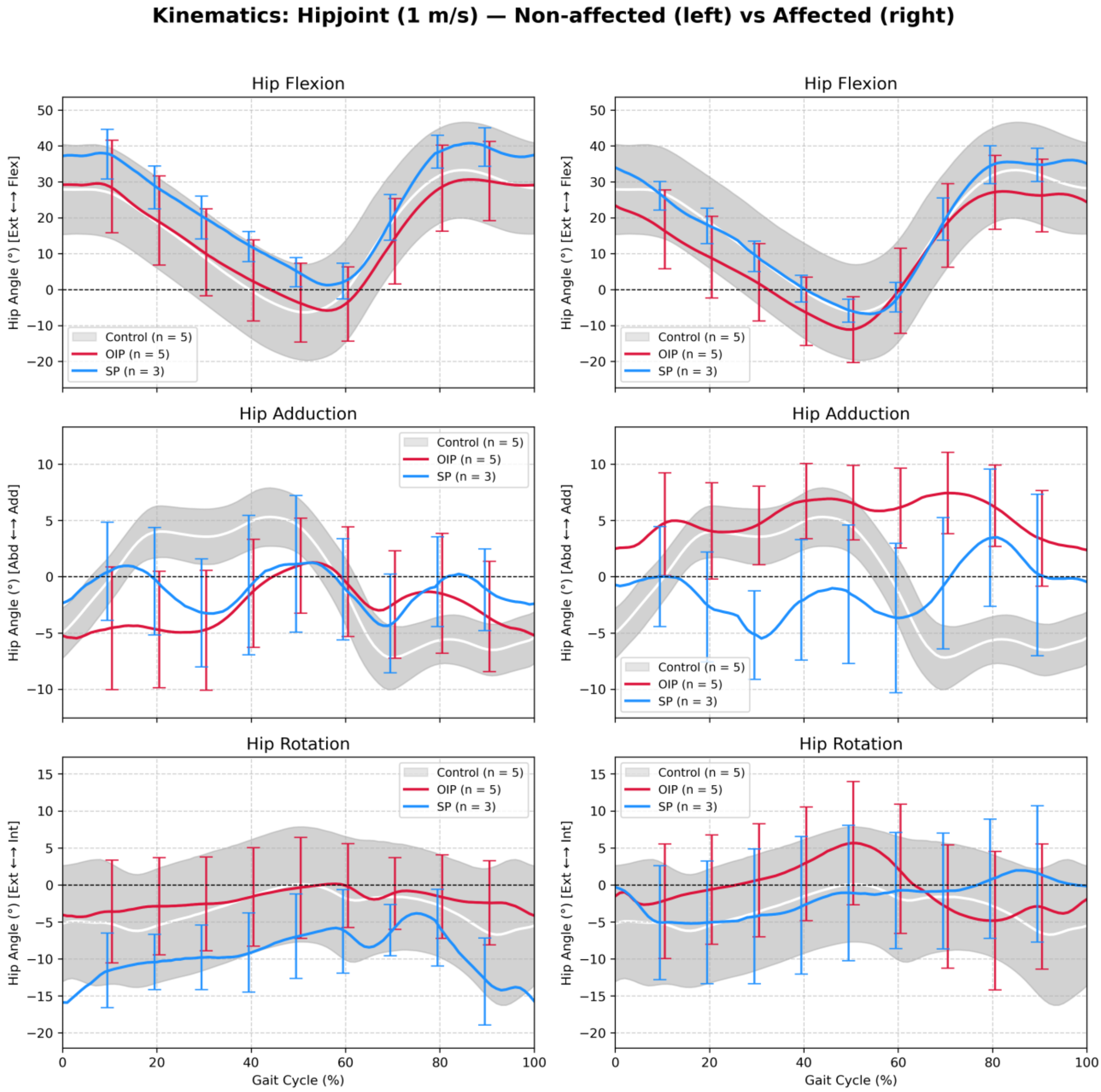

Figure 17: Hip joint kinematics at imposed speed (1 m/s) for healthy controls (grey, n = 5), OIP users (red, n = 5), and SP users (blue, n = 3). Left: non-affected side; Right: affected side. Rows show hip flexion/extension, adduction/abduction, and internal/external rotation across the gait cycle.

Appendix B2. Kinematics Knee, Ankle and Trunk (1 m/s)

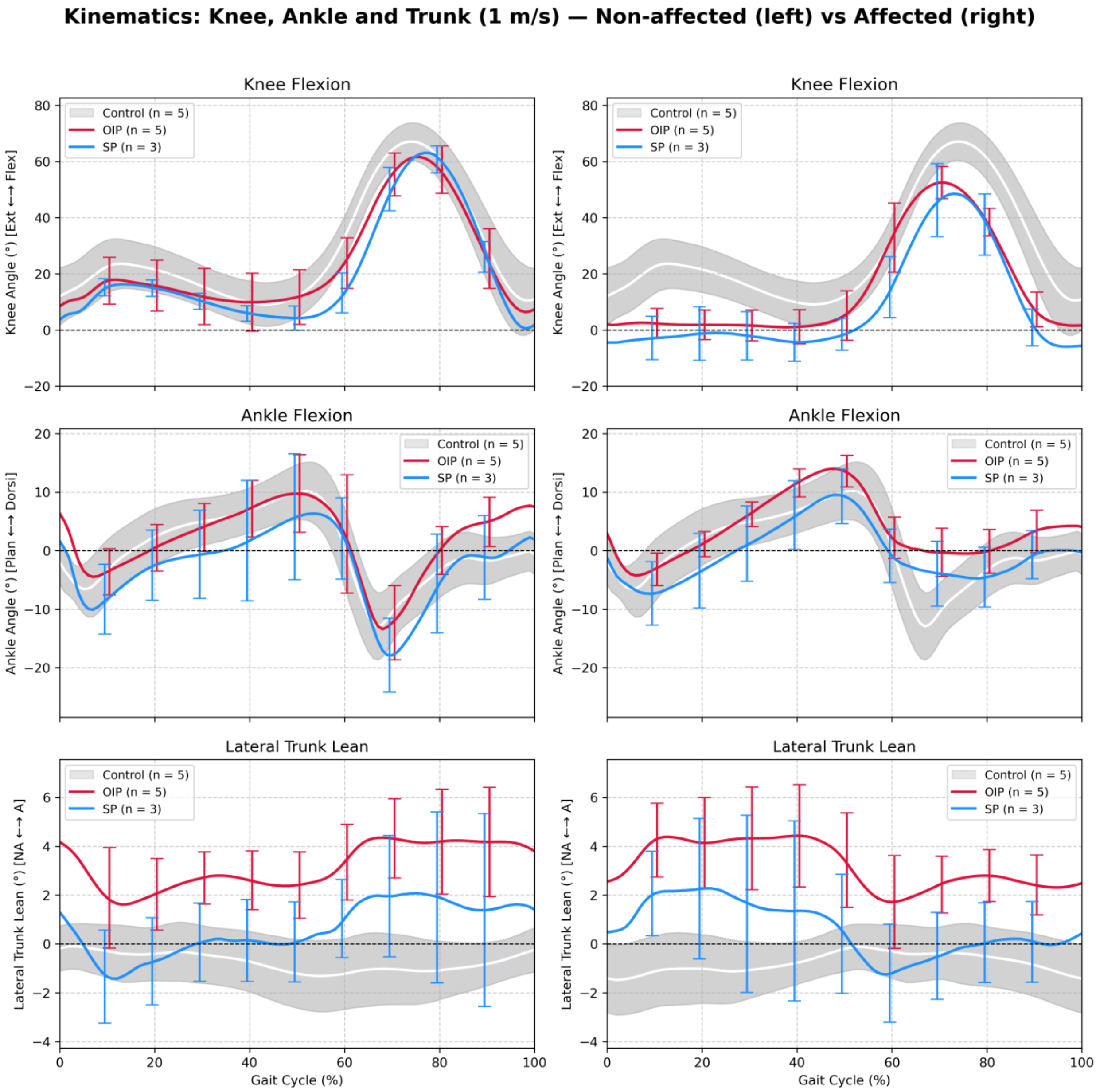

Figure 18: Knee, ankle and trunk kinematics at imposed speed (1 m/s) for healthy controls (grey, n = 5), OIP users (red, n = 5), and SP users (blue, n = 3). Left: non-affected side; Right: affected side. Rows show knee flexion/extension, ankle dorsi-/plantarflexion, and lateral trunk lean.

Appendix B3. Kinetics Hip joint (1 m/s)

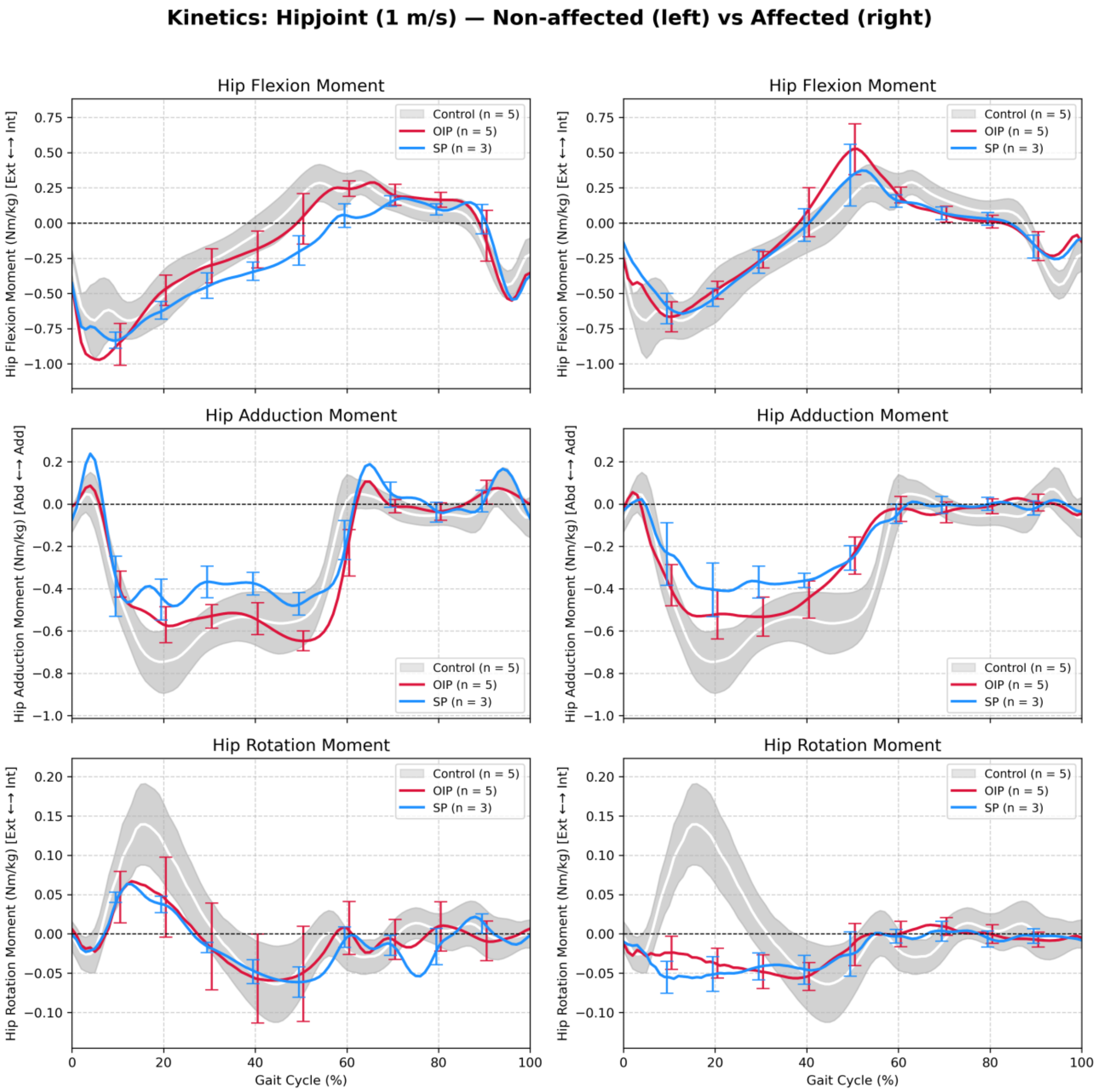

Figure 19: Hip joint kinetics at imposed speed (1 m/s) for controls (grey, n = 5), OIP (red, n = 5), and SP (blue, n = 3). Left: non-affected; Right: affected. Rows show hip flexion, adduction, and rotation moments across the gait cycle.

Appendix B4. Kinetics Knee and Ankle (1 m/s)

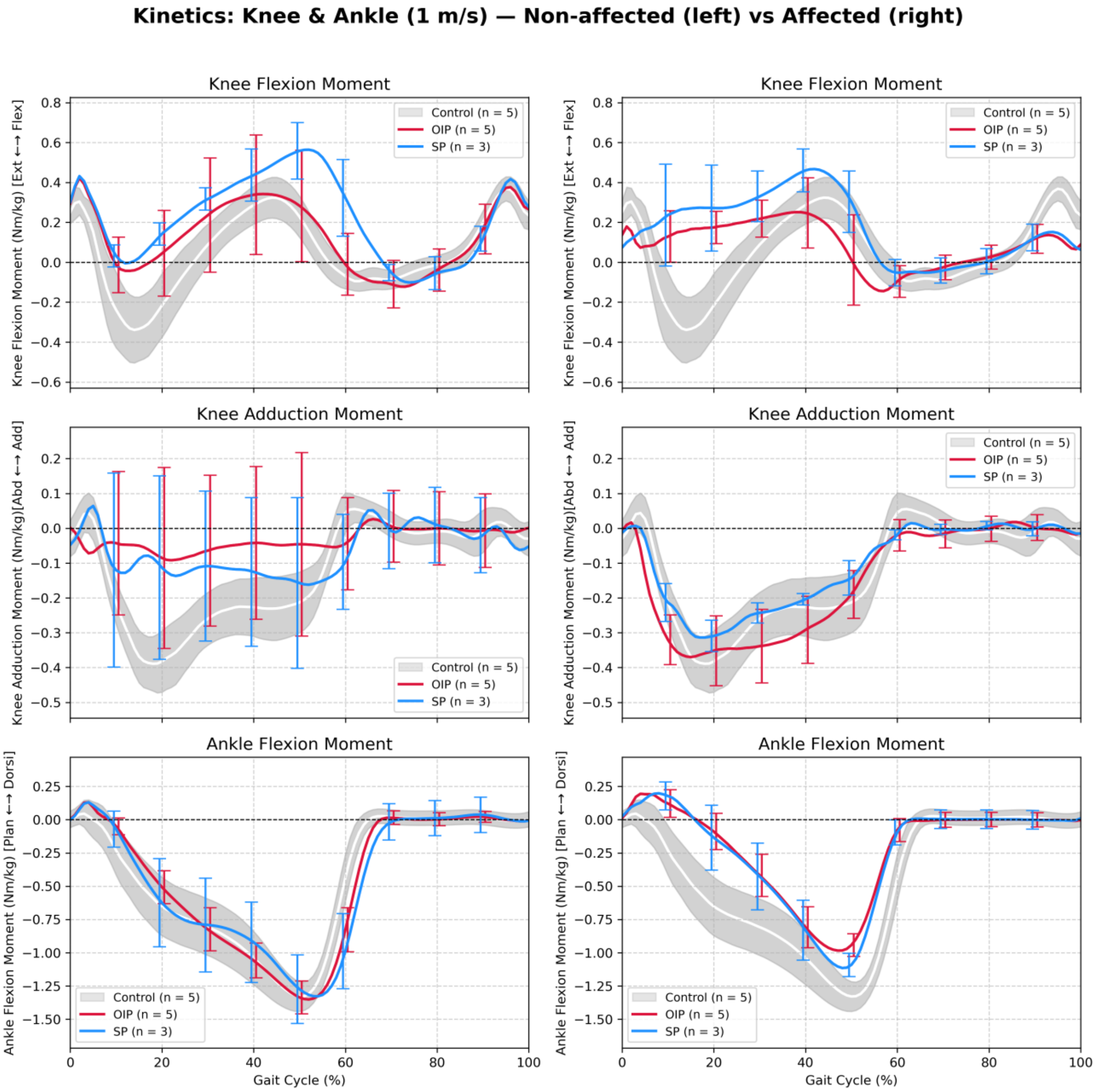

Figure 20: Knee and ankle joint kinetics at imposed speed (1 m/s) for controls (grey, n = 5), OIP (red, n = 5), and SP (blue, n = 3). Left: non-affected; Right: affected. Rows show knee flexion, knee adduction, and ankle flexion moments across the gait cycle.